Linear Transceiver Design for an Amplify-and-Forward Relay Based on the MBER Criterion

Amit Kumar Dutta, *Student Member, IEEE*, K. V. S. Hari, *Senior Member, IEEE*, and Lajos Hanzo, *Fellow, IEEE*

***Abstract*—A design methodology based on the Minimum Bit Error Ratio (MBER) framework is proposed for a non-regenerative Multiple-Input Multiple-Output (MIMO) relay-aided system to determine various linear parameters. We consider both the Relay-Destination (RD) as well as the Source-Relay-Destination (SRD) link design based on this MBER framework, including the precoder, the Amplify-and-Forward (AF) matrix and the equalizer matrix of our system. It has been shown in the previous literature that MBER based communication systems are capable of reducing the Bit-Error-Ratio (BER) compared to their Linear Minimum Mean Square Error (LMMSE) based counterparts. We design a novel relay-aided system using various signal constellations, ranging from QPSK to the general M-QAM and M-PSK constellations. Finally, we propose its sub-optimal versions for reducing the computational complexity imposed. Our simulation results demonstrate that the proposed scheme indeed achieves a significant BER reduction over the existing LMMSE scheme.**

***Index Terms*—Minimum bit error ratio (MBER), linear minimum mean square error (LMMSE), Relay, multiple-input multiple-output (MIMO), singular-value-decomposition (SVD).**

I. Introduction

RELAY-BASED communication systems have enjoyed considerable research attention due to their ability to provide a substantial spatial diversity gain with the aid of distributed nodes, hence potentially extending the coverage area and/or for reducing the transmit power [1], [2]. A pair of key protocols has been conceived for relay-aided systems, namely the regenerative [3], [4] and the non-regenerative [5], [6] protocols. In the regenerative scenario, the relay node (RN) decodes the signal and then forwards it after amplification to the destination node (DN) (also known as a decode-forward relay), while maintaining the same total relay- plus source-power as the original non-relaying scheme. By contrast, in the case of non-regenerative relaying, the RN only amplifies the signal received from the source node (SN) and then forwards it to the DN without any decoding (also known as an amplify-and-forward relay), again, without increasing the power of the original direct SN-DN pair. Non-regenerative relaying is invoked for applications, where both low latency and low complexity are required.

Multiple-input multiple-output (MIMO) techniques may be beneficially combined with relaying for further increasing both the attainable spectral efficiency and the signal reliability. The non-regenerative relay involves the design of both the Amplify-and-Forward (AF) matrix at the RN and the linear equalizer design at the DN, or any precoder matrix at the SN, subject to the above total SN and (or) RN power constraints. Various Cost Functions (CF) have been proposed for optimizing these matrices, such as the Linear Minimum Mean Square Error (LMMSE) [7]–[10] and the Maximum Capacity (MC) [11], [12] CFs, etc. However, the direct minimization of the Bit-Error-Ratio (BER) at the DN has not as yet been fully explored in the context of designing the various parameters of non-regenerative MIMO-aided relaying, although a BER based RN design was proposed In reply to: [13] for a single-antenna scenario. Hence, the work in [13] does not deal with the design of precoder, AF and linear equalizers as matrices due to the consideration of single antenna at SN, RN and DN. Though, a Minimum Bit Error Ratio (MBER) CF based MIMO-aided relay design [14] was provided for a cooperative, non-regenerative relay employing distributed space time coding, it was based on the classic BPSK signal sets. This work assumes the power allocation matrix to be diagonal and no RN power constraint was used in the optimization problem. In this case of [14], the relay power was normalized after determining the diagonal AF and precoder matrices with unconstrained optimization problem, which leads to a sub-optimal solution.

The benefit of MBER-based linear system design has been well studied in literature. To elaborate a little further, the MBER CF directly minimizes the BER [15]. Previous literature has shown that a sophisticated system design based on this criterion is capable of outperforming its LMMSE counterpart in terms of the attainable BER. Owing to its benefits, it has been used for the design of a linear equalizer [15], for the precoder matrix [16] and for various other MIMO, SDMA as well as OFDM systems conceived for achieving the best BER performance [17]–[19] at the of higher computational complexity. MBER based linear receiver design has also been shown to be very effective in terms of BER performance in the rank-deficient case, where conventional LMMSE-based receiver fails to perform significantly [20].

Manuscript received January 30, 2014; revised June 26, 2014; accepted August 12, 2014. The associate editor coordinating the review of this paper and approving it for publication was M. Uysal.

A. K. Dutta and K. V. S. Hari are with the Department of Electrical Communication Engineering, Indian Institute of Science, Bangalore 560012, India (e-mail: amitkdatta@ece.iisc.ernet.in; hari@ece.iisc.ernet.in).

L. Hanzo is with the Department of Electronics and Computer Science, University of Southampton, Southampton SO17 1BJ, U.K. (e-mail: lh@ecs.soton.ac.uk).

Digital Object Identifier 10.1109/TCOMM.2014.2350973

Scope and contribution: Against this background based on the MBER CF, we design of a new non-regenerative MIMO-aided relaying system, which comprises a SN, a RN and a DN. We assume a half duplex system at the RN, where one time slot is used for receiving from the SN and another for forwarding it to the DN. No SN-RN transmission takes place during the RN-DN transmission. In this work, we consider the joint design of the SN's transmit precoder, the RN's AF matrix and the DN's linear equalizer matrix based on the MBER CF subject to the above total RN-SN power constraints. The performance of the proposed scheme is evaluated and compared to that of the existing LMMSE based method. The main contributions of this treatise are as follows:

1) A CF is conceived for the design of the RN-DN and the SN-RN-DN links of a non-regenerative relaying system based on the MBER CF subject to the SN and (or) RN power constraints. The MBER CF is formulated for various data constellations, ranging from BPSK to the general M-QAM and M-PSK constellations. Naturally, the specific choice of the constellation fundamentally influences the MBER CF [15], [17]–[19]. We jointly determine the precoder, AF and equalizer matrices based on this MBER CF under a source and relay power constraint. The existing MIMO MBER solutions are designed for unconstrained scenarios and hence this constrained MBER optimization poses specific challenges. Therefore, we have conceived both the heuristic constrained binary Genetic Algorithm (GA) [21] and the Projected Steepest Descent (PSD) [22] algorithm for determining these parameters.
2) A suboptimal method is also proposed for reducing the number of variables using the Singular-Value-Decomposition (SVD) approach, which allows the optimization problem to be decomposed into multiple parallel optimization problems. The key contribution here is that we propose to split the complete constrained optimization problem into unconstrained parallel optimization problems except for one of the cases.
3) The Cost Function (CF) of M-PSK constellation has been approximated for the sake of conceiving a more tractable form for the MIMO-aided relaying system considered. This approximation can also be used for classic MIMO scenarios.
4) An impediment of the MBER CF is however its high computational complexity compared to its LMMSE counterpart [15]. To mitigate this, we have conceived a low-complexity data detection scheme for the MBER method with the aid of the phase rotation of the constellation in the context of rotationally invariant QPSK and M-PSK constellations. This scheme can be equally applicable to any other MIMO system design based on the MBER criterion.
5) An approximate complexity analysis is performed for the MBER scheme under various constrained optimization methods such as the GA and PSD. This step-by-step analysis may be readily applied to other MBER solutions.

Notation: Bold upper and lower case letters denote matrices and vectors, respectively. The superscripts $(\cdot)^T$ and $(\cdot)^H$ denote the transpose and the conjugate transpose of a matrix, respectively. $\mathbb{E}[\cdot]$ denotes the expectation, while $\mathbf{I}_N$ denotes a $(N \times N)$-element identity matrix. $Tr[\cdot]$ represents the trace of a matrix. A diagonal matrix is denoted by $diag\{a_1, a_2, \ldots, a_N\}$, where a_n denotes the nth diagonal element. $vec(\mathbf{A})$ is the vectorization of the matrix $\mathbf{A}$ with columns stacked one-by-one.

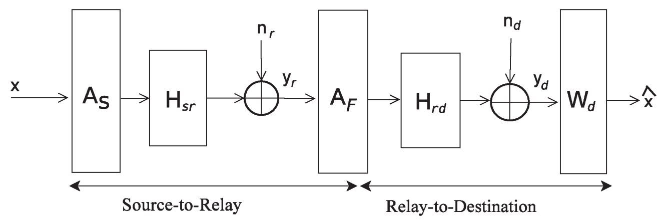

Fig. 1. Single relay system with multiple input-output antennas at source, relay, and destination.

II. System Model

We consider a communication system consisting of a SN, a RN and a DN having N_s, N_r, and N_d antennas, respectively, as shown in Fig. 1. It is assumed that there is no Line-Of-Sight (LOS) component between the SN and the DN. Both the SN-RN and the RN-DN channel matrices are assumed to be those of flat-fading channels, which are denoted as $\mathbf{H}_{sr} \in \mathbb{C}^{N_r \times N_s}$ and $\mathbf{H}_{rd} \in \mathbb{C}^{N_d \times N_r}$, respectively. The symbol vector transmitted from the SN before precoding is denoted as $\mathbf{x} \in \mathbb{C}^{N_x \times 1}$ with N_x being the length of the input vector. We assume $\mathbf{A}_S \in \mathbb{C}^{N_S \times N_x}$ to be the precoding matrix at the SN. The average transmitted power is constrained to $P_t = \mathbb{E}[\mathbf{s}^H\mathbf{s}]$ with $\mathbf{s} \triangleq \mathbf{A}_S\mathbf{x}$, which is assumed to be the same for all symbols at the SN. Hence, we have the transmit power constraint as $P_t \triangleq \mathbb{E}\|\mathbf{A}_S\mathbf{x}\|^2 = \sigma_x^2 Tr(\mathbf{A}_S\mathbf{A}_S^H)$ and the transmit data covariance matrix is $\mathbf{R}_S \triangleq \mathbb{E}(\mathbf{s}\mathbf{s}^H) = (P_t/N_x)(\mathbf{A}_S\mathbf{A}_S^H)$, where $\sigma_x^2 = (P_t/N_x)$ is the signal power of each data x_i. The noise vectors at the RN and the DN are $\mathbf{n}_r \in \mathbb{C}^{N_r \times 1}$ and $\mathbf{n}_d \in \mathbb{C}^{N_d \times 1}$, respectively, which are assumed to be zero mean, circularly symmetric complex i.i.d Gaussian vectors having the covariance matrices of $\sigma_r^2\mathbf{I}_{N_r}$ and $\sigma_d^2\mathbf{I}_{N_d}$, respectively. We consider a classic half duplex system. Hence, in the first time slot, the SN transmits a source vector $\mathbf{s}$ and the vector $\mathbf{y}_r \in \mathbb{C}^{N_r \times 1}$, received at the RN is given by,

$$\mathbf{y}_r = \mathbf{H}_{sr}\mathbf{s} + \mathbf{n}_r. \tag{1}$$

During the next time slot, the relay would multiply the received vector $\mathbf{y}_r$ with the AF matrix $\mathbf{A}_F \in \mathbb{C}^{N_r \times N_r}$ and then forwards it to the DN. Let us assume that $\mathbf{y}_F \triangleq \mathbf{A}_F\mathbf{y}_r = \mathbf{A}_F(\mathbf{H}_{sr}\mathbf{s} + \mathbf{n}_r)$. We impose the RN transmit power restriction of $\mathbb{E}[\mathbf{y}_F^H\mathbf{y}_F] \le P_r$, where P_r is the RN's transmit power. Assuming that the SN's transmitted signal and the noise are independent, the RN's power can be calculated as,

$$\begin{aligned}\mathbb{E}\left[\mathbf{y}_f^H\mathbf{y}_f\right] &= Tr\left\{\mathbb{E}\left(\mathbf{A_F}(\mathbf{H}_{sr}\mathbf{s} + \mathbf{n}_r)(\mathbf{H}_{sr}\mathbf{s} + \mathbf{n}_r)^H\mathbf{A}_F^H\right)\right\}\\ &= Tr\left\{\mathbf{A}_F\left(\sigma_x^2\mathbf{H}_{sr}\mathbf{A}_S\mathbf{A}_S^H\mathbf{H}_{sr}^H + \sigma_r^2\mathbf{I}_{N_r}\right)\mathbf{A}_F^H\right\}\\ &\le P_r,\end{aligned} \tag{2}$$

TABLE I
REQUIREMENT OF CSI AT VARIOUS NODES FOR MBER CRITERION BASED RELAY DESIGN

Relay design type	*SN*	*RN*	*DN*
RN-DN		$\mathbf{H}_{sr}$, $\mathbf{H}_{rd}$	$\mathbf{H}_{rd}$
SN-RN-DN (Sub-optimal)	$\mathbf{H}_{sr}$	$\mathbf{H}_{sr}$, $\mathbf{H}_{rd}$	$\mathbf{H}_{rd}$
SN-RN-DN (Optimal)		$\mathbf{H}_{sr}$, $\mathbf{H}_{rd}$	$\mathbf{H}_{rd}$

where $\mathbb{E}\{\mathbf{x}\mathbf{x}^H\} = \sigma_x^2 \mathbf{I}_{N_x}$. Now, the signal received at the DN, $\mathbf{y}_d \in \mathbb{C}^{N_d \times 1}$ is obtained as,

$$\begin{aligned}\mathbf{y}_d &= \mathbf{H}_{rd}\mathbf{y}_f + \mathbf{n}_d \\ &= \mathbf{H}_{rd}\mathbf{A}_F\left(\mathbf{H}_{sr}\mathbf{s} + \mathbf{n}_r\right) + \mathbf{n}_d \\ &= \{\mathbf{H}_{rd}\mathbf{A}_F\mathbf{H}_{sr}\mathbf{A}_S\}\,\mathbf{x} + \{\mathbf{H}_{rd}\mathbf{A}_F\mathbf{n}_r + \mathbf{n}_d\} \\ &\triangleq \mathbf{H}\mathbf{x} + \mathbf{n},\end{aligned} \tag{3}$$

where $\mathbf{H} \triangleq \mathbf{H}_{rd}\mathbf{A}_F\mathbf{H}_{sr}\mathbf{A}_S$ and $\mathbf{n} \triangleq \mathbf{H}_{rd}\mathbf{A}_F\mathbf{n}_r + \mathbf{n}_d$. The new effective noise vector $\mathbf{n}$ is a colored zero-mean Gaussian vector with the distribution of $CN(\mathbf{0}, \mathbf{C}_n)$, where $\mathbf{C}_n \in \mathbb{C}^{N_d \times N_d}$ is the new noise covariance matrix, which may be expressed as,

$$\begin{aligned}\mathbf{C}_n &= \mathbb{E}[\mathbf{n}\mathbf{n}^H] \\ &= \sigma_d^2\mathbf{I}_{N_d} + \sigma_r^2\mathbf{H}_{rd}\mathbf{A}_F\mathbf{A}_F^H\mathbf{H}_{rd}^H.\end{aligned} \tag{4}$$

At the DN, we employ a linear equalizer for detecting the transmitted symbol $\mathbf{x}$. We assume that the equalizer matrix at the DN is $\mathbf{W}_d \in \mathbb{C}^{N_x \times N_d}$, hence the estimated value of $\mathbf{x}$ is $\hat{\mathbf{x}} = \mathbf{W}_d^H\mathbf{y}_d$.

Note: The RN determines the $\mathbf{A}_S$, $\mathbf{A}_F$ and $\mathbf{W}_d$ matrices jointly. Thus, we assume that the RN has the complete knowledge of $\mathbf{H}_{sr}$ and $\mathbf{H}_{rd}$, while the DN knows only $\mathbf{H}_{rd}$ and feeds it back to the RN through a reliable communication channel. The SN has to know the matrix $\mathbf{H}_{sr}$ only for the case of the sub-optimal SN-RN-DN (SRD) relay design to be described later. We refer "sub-optimal", when Singular-Value-Decomposition (SVD) based structure is assumed for AF and source precoder matrices. In this case, only the singular values of these matrices need to be determined. By contrast, "optimal" refers to the case, where full complex AF and source precoder matrices need to be determined. Thus, for "optimal" case, SN need not to know the $\mathbf{H}_{sr}$ as the whole solution of the precoder will be sent back to SN by RN. For the sub-optimal case, the SN needs to reconstruct the precoder matrix from the SVD component of the $\mathbf{H}_{sr}$ matrix. Table I shows the parameter knowledge requirements at different nodes, which are consistent with [9], except for our proposed optimal SN-RN-DN link design. We first develop the RN-DN link and then extend it to the SN-RN-DN link. For the RN-DN system, only the matrices $\mathbf{A}_F$ and $\mathbf{W}_d$ have to be determined subject to the above RN power constraints. By contrast, for the SN-RN-DN system, the matrices $\mathbf{A}_S$, $\mathbf{A}_F$ and $\mathbf{W}_d$ are determined subject to both the SN and the RN power constraints.

III. MBER Based Relay-Destination Design

We first consider the RN-DN link design, which involves the design of both the AF matrix $\mathbf{A}_F$ and of the equalizer matrix $\mathbf{W}_d$. Various existing CFs, such as the LMMSE [7], the Maximum Capacity (MC) [11] have been considered to design both $\mathbf{A}_F$ and $\mathbf{W}_d$. In this treatise, we propose a solution based on the MBER CF for jointly determining these matrices. For the RN-DN link, the precoder matrix $\mathbf{A}_S$ is fixed to $\mathbf{I}_{N_s}$ along with $N_s = N_x$. The total transmitted power is fixed to $P_t = \sigma_x^2 N_s$. The signals received at the RN and the DN are $\mathbf{y}_r = \mathbf{H}_{sr}\mathbf{x} + \mathbf{n}_r$ and $\mathbf{y}_d = \mathbf{H}_{rd}\mathbf{A}_F\mathbf{H}_{sr}\mathbf{x} + \mathbf{H}_{rd}\mathbf{A}_F\mathbf{n}_r + \mathbf{n}_d$, respectively. The RN's power becomes $Tr\{\mathbf{A}_F(\sigma_x^2\mathbf{H}_{sr}\mathbf{H}_{sr}^H + \sigma_r^2\mathbf{I}_{N_r})\mathbf{A}_F^H\}$. In the current context, the MBER CF directly minimizes the BER of the system at the DN. We first consider the CF based on the BPSK constellation and then we extend it to the M-QAM and M-PSK constellations.

Note: We will be formulating the cost function (CF) as the symbol error ratio (SER). With a slight inaccuracy of terminology, we refer to the MBER as that of minimizing the SER in the subsequent sections. It is to be noted that minimizing SER will also lead to minimization of BER as $BER \approx SER/\log_2(M)$ for most of the constellations [23].

A. Cost Function

Let us assume that $P_{e,i}$ denotes the SER, when detecting x_i (the ith component of $\mathbf{x}$) at the DN. If every x_i is detected independently, the average probability of a symbol error associated with detecting the complete vector $\mathbf{x}$ is given by,

$$P_e = \frac{1}{N_s}\sum_{i=1}^{N_s} P_{e,i}. \tag{5}$$

We constrain the RN's transmission power to P_r and formulate $P_{e,i}$ associated with various constellations. Furthermore, we would simplify the expression of $P_{e,i}$ using various sub-optimal approaches. The optimization problem is stated as follows:

$$\begin{aligned}&\mathbf{A}_F^{mber}, \mathbf{W}_d^{mber} = \underset{\mathbf{A}_F, \mathbf{W}_d}{arg}\ \min\ P_e(\mathbf{A}_F, \mathbf{W}_d) \\ &s.t\ Tr\left\{\mathbf{A}_F\left(\sigma_x^2\mathbf{H}_{sr}\mathbf{H}_{sr}^H + \sigma_r^2\mathbf{I}_{N_r}\right)\mathbf{A}_F^H\right\} \le P_r.\end{aligned} \tag{6}$$

Note: Equation (6) describes a constrained optimization problem, where the constraint is with respect to the RN's transmitter power. Here, all $P_{e,i}$ for $i = 1, 2 \ldots, N_s$ are optimized together to arrive at the optimized $\mathbf{A}_F$ and $\mathbf{W}_d$ matrices. Explicitly, Equation (6) is simultaneously optimized over $(N_r^2 + N_s \times N_d)$ number of complex-valued variables. This is because the $\mathbf{A}_F$ matrix has N_r^2 number of complex entries, while the $\mathbf{W}_d$ matrix has $(N_s \times N_d)$ complex entries. Therefore, the related optimization problem has a high computational complexity. Hence, we now propose a suboptimal technique for reducing the number of variables to be optimized.

1) Sub-Optimal Approaches for Reducing Both the Number of Variables and the Complexity: Let us first decompose $\mathbf{H}_{sr}$ and $\mathbf{H}_{rd}$ using the Singular Value Decomposition (SVD) as $\mathbf{H}_{sr} = \mathbf{U}_1\mathbf{\Sigma}_{sr}\mathbf{V}_1^H$ and $\mathbf{H}_{rd} = \mathbf{U}_2\mathbf{\Sigma}_{rd}\mathbf{V}_2^H$ respectively, where $\mathbf{U}_1 \in \mathbb{C}^{N_r \times N_r}$, $\mathbf{V}_1 \in \mathbb{C}^{N_s \times N_s}$, $\mathbf{U}_2 \in \mathbb{C}^{N_d \times N_d}$, $\mathbf{V}_2 \in \mathbb{C}^{N_r \times N_r}$ are unitary matrices, whereas $\mathbf{\Sigma}_{sr} \in \mathbb{R}^{N_r \times N_S}$ and $\mathbf{\Sigma}_{rd} \in \mathbb{R}^{N_d \times N_r}$ are matrices having singular values of $\sigma_{sr,i}$ for $i = 1, 2, \ldots, \min(N_r, N_s)$ and $\sigma_{rd,i}$ for $i = 1, 2, \ldots, \min(N_d, N_r)$ in a descending order on the main diagonal, respectively. We also assume that $\mathbf{w}_i$ is the ith column of $\mathbf{W}_d$ for $i = 0, 1, \ldots, N_d - 1$.

We now propose a pair of computational complexity reduction techniques.

1) We use the SVD of the matrix $\mathbf{A}_F$, which has been shown to be optimal in the Mean Square Error (MSE) sense [7]. However, this decomposition may not be optimal in the MBER sense. The assumed structure of $\mathbf{A}_F$ is defined as,

$$\mathbf{A}_F \triangleq \mathbf{V}_2 \mathbf{\Sigma}_F \mathbf{U}_1^H \tag{7}$$

where the unitary matrices $\mathbf{V}_2$ and $\mathbf{U}_1$ have been defined earlier. Furthermore, $\mathbf{\Sigma}_F \in \mathbb{R}^{N_r \times 1}$ is the singular value matrix of $\mathbf{A}_F$, which has the singular values of $\sigma_{f,i}$ for $i = 1, 2, \ldots, N_r$. This reduces the N_r^2 number of complex variables to just N_r real variables.

2) We propose to optimize each $P_{e,i}$ in parallel. This reduces the optimization complexity for each index i. We propose furthermore that for the k^{th} index $i = k$, $P_{e,k}$ is optimized with respect to both $\mathbf{\Sigma}_F$ and $\mathbf{w}_k$. The obtained $\mathbf{\Sigma}_F$ is then used for the rest of the $P_{e,i}$ values for $i = 1, 2, 3, \ldots, k-1, k+1, \ldots, N_s$ as a given parameter. It is noted that the RN's power constraint is not a function of any of the equalizers for $i = 1, 2, 3, \ldots, k-1, k+1, \ldots, N_s$, hence the RN's power constraint is not considered thereafter. As a benefit, a valuable computational complexity reduction is achieved, since we only have to deal with $(N_r + N_d)$ number of complex variables for $i = k$ and then only with N_d complex variables for rest of i values without any RN power constraint. Furthermore, for $i = 1, 2, 3, \ldots, k-1, k+1, \ldots, N_s$ onward, the computation of $\mathbf{w}_i$ can be performed in parallel, which facilitates the design of a larger chip capable of operating at a higher bit-rate, regardless of the specific choice of optimization method.

By exploiting the SVD structure based assumption concerning $\mathbf{A}_F$, $\mathbf{H}$ can be reduced to

$$\begin{aligned}
\mathbf{H} &= \mathbf{H}_{rd} \mathbf{A}_F \mathbf{H}_{sr} \\
&= \mathbf{U}_2 \mathbf{\Sigma}_{rd} \mathbf{V2}^H \mathbf{V}_2 \mathbf{\Sigma}_F \mathbf{U1}^H \mathbf{U}_1 \mathbf{\Sigma}_{sr} \mathbf{V1}^H \\
&= \mathbf{U}_2 \mathbf{\Sigma}_{rd} \mathbf{\Sigma}_F \mathbf{\Sigma}_{sr} \mathbf{V1}^H \\
&\triangleq \mathbf{U}_2 \mathbf{\Sigma} \mathbf{V}_1^H,
\end{aligned} \tag{8}$$

where $\mathbf{\Sigma} \triangleq \mathbf{\Sigma}_{rd} \mathbf{\Sigma}_F \mathbf{\Sigma}_{sr}$. Let us now compute the RN's power under the assumed structure of $\mathbf{A}_F$ as follows

$$\begin{aligned}
\mathbb{E}\left[\mathbf{y}_f^H \mathbf{y}_f\right] &= Tr\left\{\mathbf{A}_F \left(\sigma_x^2 \mathbf{H}_{sr} \mathbf{H}_{sr}^H + \sigma_r^2 \mathbf{I}_{N_r}\right) \mathbf{A}_F^H\right\} \\
&= Tr\left\{\mathbf{V}_2 \mathbf{\Sigma}_F \left(\sigma_x^2 \mathbf{\Sigma}_{sr} \mathbf{\Sigma}_{sr}^H + \sigma_r^2 \mathbf{I}_{N_r}\right) \mathbf{\Sigma}_F^H \mathbf{V}_2^H\right\} \\
&= Tr\left\{\mathbf{\Sigma}_F \left(\sigma_x^2 \mathbf{\Sigma}_{sr} \mathbf{\Sigma}_{sr}^H + \sigma_r^2 \mathbf{I}_{N_r}\right) \mathbf{\Sigma}_F^H\right\} \\
&= \sum_{i=1}^{N_r} \sigma_{f,i}^2 \left(\sigma_x^2 \sigma_{sr,i}^2 + \sigma_r^2\right) \leq P_r.
\end{aligned} \tag{9}$$

Explicitly, the RN's power constraint becomes less complex, since it does not involve any complex-valued matrix operations. In a similar way, we now re-calculate the covariance matrix $\mathbf{C}_n$ of the composite noise, as perceived at the DN. Let us assume that $\mathbf{A} \triangleq \mathbf{H}_{rd} \mathbf{A}_F \mathbf{A}_F^H \mathbf{H}_{rd}$. Thus, we calculate $\mathbf{A}$ as follows

$$\begin{aligned}
\mathbf{A} &= \mathbf{H}_{rd} \mathbf{A}_F \mathbf{A}_F^H \mathbf{H}_{rd} \\
&= \mathbf{U}_2 \mathbf{\Sigma}_{rd} \mathbf{V}_2^H \mathbf{V}_2 \mathbf{\Sigma}_F \mathbf{\Sigma}_F^H \mathbf{V}_2^H \mathbf{V}_2 \mathbf{\Sigma}_{rd}^H \mathbf{U}_2^H \\
&= \mathbf{U}_2 \mathbf{\Sigma}_{rd} \mathbf{\Sigma}_F \mathbf{\Sigma}_F^H \mathbf{\Sigma}_{rd}^H \mathbf{U}_2^H \\
&\triangleq \mathbf{U}_2 \mathbf{\Sigma}_A \mathbf{U}_2^H,
\end{aligned} \tag{10}$$

where $\mathbf{\Sigma}_A \triangleq \mathbf{\Sigma}_{rd} \mathbf{\Sigma}_F \mathbf{\Sigma}_F^H \mathbf{\Sigma}_{rd}^H$. Upon substituting Equation (10) into Equation (4), we arrive at $\mathbf{C}_n = \sigma_d^2 \mathbf{I}_{N_d} + \sigma_r^2 \mathbf{U}_2 \mathbf{\Sigma}_A \mathbf{U}_2^H$. Our new optimization problem is then redefined as follows

$$\begin{aligned}
&\text{For i = k :} \\
&\mathbf{\Sigma}_F^{mber}, \mathbf{w}_k^{mber} = \underset{\mathbf{\Sigma}_F, \mathbf{w}_k}{arg \; \min} \; P_{e,k}(\mathbf{\Sigma}_F, \mathbf{w}_k) \\
&\qquad\qquad s.t \sum_{i=1}^{N_r} \sigma_{f,i}^2 \left(\sigma_x^2 \sigma_{sr,i}^2 + \sigma_r^2\right) \leq P_r.
\end{aligned} \tag{11}$$

$$\begin{aligned}
&\text{For i = 1, 2, 3, \ldots, k - 1, k + 1, \ldots, N_s :} \\
&\mathbf{w}_i^{mber} = \underset{\mathbf{w}_i}{arg \min} \; P_{e,i}(\mathbf{\Sigma}_F^{mber}, \mathbf{w}_i).
\end{aligned} \tag{12}$$

2) MBER CF Associated With the BPSK Constellation: We first formulate the MBER CF for the BPSK constellation for the sake of conceptual simplicity and then extend it to the M-QAM and M-PSK constellations. Let us assume that $\mathbf{w}_i$ is the ith column of the DN's equalizer matrix $\mathbf{W}_d$. If $\hat{x}_i$ is the estimate of x_i for the BPSK constellation, we arrive at the expression of $P_{e,i}^{BPSK}$ as follows [15]:

$$\begin{aligned}
P_{e,i}^{BPSK} &= P_r\left\{x_i \Re\{\hat{x}_i\} < 0\right\} \\
&= P_r\left\{\Re\{x_i (\mathbf{w}_i)^H \mathbf{H}\mathbf{x} + x_i (\mathbf{w}_i)^H \mathbf{n}\} < 0\right\} \\
&= \mathbb{E}_{\mathbf{x}}\left[P_r\left\{\Re\{x_i (\mathbf{w}_i)^H \mathbf{H}\mathbf{x} + x_i (\mathbf{w}_i)^H \mathbf{n}\} < 0\right\} |\mathbf{x}\right] \\
&= \mathbb{E}_{\mathbf{x}}\left[Q\left(\frac{\Re\left[(\mathbf{w}_i)^H \mathbf{H}\mathbf{x} x_i\right]}{\sqrt{\frac{1}{2}(\mathbf{w}_i)^H \mathbf{C}_n \mathbf{w}_i}}\right)\right] \\
&= \frac{1}{L} \sum_{j=1}^{L} Q\left(\frac{\Re\left[(\mathbf{w}_i)^H \mathbf{H}\mathbf{x}_j x_i\right]}{\sqrt{\frac{1}{2}(\mathbf{w}_i)^H \mathbf{C}_n \mathbf{w}_i}}\right),
\end{aligned} \tag{13}$$

where $L = 2^{N_s}$ represents the total number of unique realizations of $\mathbf{x}$, while $\mathbf{x}_j$ is the jth such realization of $\mathbf{x}$.

3) The MBER CF Associated With the M-QAM Constellation: For the M-QAM constellation, we assume that the distance between any two adjacent constellation points along either the real or the imaginary axis is $2a$ for $a > 0$.

The M-QAM constellation can thus be interpreted as a pair of PAM sequences of length $\sqrt{M}$ along the real and imaginary axes. Thus, the SER of the M-QAM constellation is derived as,

$$P_{e,i}^{QAM} = 1 - P_{c,i}^{R} \cdot P_{c,i}^{I} \tag{14}$$

where $P_{c,i}^{R}$, $P_{c,i}^{I}$ are the probability of correct decision for the QAM signal along the real and imaginary axes, respectively. For computational simplicity, we assume that the decision region of each point along either the real or imaginary axis is bounded by the length $2a$, though the terminal points have larger range for decision region. This way, we only make each decision region uniform and restrictive to an extent. Let us now define $L_1 = M^{((N_s-1)/2)}$. Now, $P_{c,i}^{R}$, $P_{c,i}^{I}$ are derived in Equations (15) and (16), respectively (see equation at bottom of page).

4) The MBER CF Associated With the M-PSK Constellation: For the M-PSK signal constellation set, each point is assumed to be on a unit circle and represented as $e^{j(2\pi m/M)}$ for $m = 0, 1, \ldots, M-1$. Note that the real and imaginary components of the DN's equalizer output noise, $\mathbf{w}_i^H \mathbf{n}$, are correlated Gaussian random variables. For computational simplicity, we invoke an approximation and we whiten the noise by assuming $\mathbf{A}_F$ to have the proposed SVD form of Equation (7). We commence by using $\mathbf{C}_n$ from Equation (4) as,

$$\mathbf{C}_n = \mathbf{\Sigma}_{rd}\mathbf{\Sigma}_F\mathbf{\Sigma}_F^T\mathbf{\Sigma}_{rd}^T + \sigma_d^2\mathbf{I}_{N_d}. \tag{17}$$

Thus, the ith diagonal element of $\mathbf{C}_n$ is $[\mathbf{C}_n]_{ii} = \sigma_d^2 + \sigma_{rd,i}^2\sigma_{f,i}^2$. The noise whitening matrix is defined as $\mathbf{C}_s \triangleq \mathbf{C}_n^{-(1/2)}$ with $[\mathbf{C}_s]_{ii} = (1/\sqrt{\sigma_d^2 + \sigma_{rd,i}^2\sigma_{f,i}^2})$. Therefore, the modified output vector received at the DN is defined as,

$$\begin{aligned}\mathbf{y}_s &= \mathbf{C}_s\mathbf{y}_d \\ &= \mathbf{C}_s\mathbf{H}\mathbf{x} + \mathbf{n}_s \\ &= \mathbf{H}_s\mathbf{x} + \mathbf{n}_s,\end{aligned} \tag{18}$$

with $\mathbf{n}_s \in \mathbb{C}^{N_s\times 1}$ being the zero-mean i.i.d Gaussian random vector with each component having a unit variance. Let us assume that $\mu_i^R \triangleq \Re\{\mathbf{w}_i^H\mathbf{H}_s\mathbf{x}\}$ and $\mu_i^I \triangleq \Im\{\mathbf{w}_i^H\mathbf{H}_s\mathbf{x}\}$, where $\mathbf{w}_i$ is the ith equalizer as defined earlier. Let furthermore r_1 and r_2 be the real and imaginary components of the equalizer output. Their joint probability is calculated as [23],

$$p_{r_1,r_2,i} = \frac{1}{2\pi\sigma^2}e^{-\left\{(r_1-\mu^R)^2+(r_2-\mu^I)^2\right\}/2\sigma^2} \tag{19}$$

where $\sigma^2 = (1/2)\mathbf{w}_i^H\mathbf{w}_i$. Let us now define $V \triangleq \sqrt{r_1^2 + r_2^2}$ and the angle $\theta \triangleq \tan^{-1}((r_2/r_1))$. Thus, the probability of θ for the ith symbol is obtained as [23]

$$p_{\theta,i} = \frac{1}{2\pi\sigma^2}e^{-\left(\mu_i^R\sin(\theta)-\mu_i^I\cos(\theta)\right)^2/2\sigma^2} \times \int_0^\infty V e^{-\left(V-\mu_i^I sin(\theta)-\mu_i^R cos(\theta)\right)^2/2\sigma^2} dV. \tag{20}$$

At the higher SNR values, an approximation has been proposed for Equation (20) in [23] as follows,

$$p_{\theta,i} \approx \frac{1}{\sqrt{2\pi\sigma^2}}\left(\mu_i^I sin(\theta) + \mu_i^R cos(\theta)\right) \times e^{-\left(\mu_i^R\sin(\theta)-\mu_i^I\cos(\theta)\right)^2/2\sigma^2}, \tag{21}$$

with $|\theta| \leq \pi/2$ and $|\theta| << 1$. Equation (21) is valid for $m = 0$. This suggests that any constellation point at the ith position of $\mathbf{x}$ can be rotated to the one corresponding to $m = 0$. Hence, we may conceive a scheme by exploiting the circular constellation of M-PSK, where the SER has to be found for the constellation point corresponding to $m = 0$. Thus, $\mathbf{w}_i$ is determined by minimizing the probability of this particular symbol error only. We then create M rotated versions of $\mathbf{y}_d$ as $\mathbf{y}_d^m = e^{-m\pi/M}\mathbf{I}_{N_d}\mathbf{y}_d$ for $m = 0, 1, \ldots, M-1$. The estimated constellation point $(\mathbf{w}_i^H\mathbf{y}_d^m)$ is then the one corresponding to any of the M number of $\mathbf{y}_d^m$ variables giving the minimum absolute angle.

$$P_{c,i}^{R} = \frac{1}{L_1}\sum_{j=1}^{L_1}\sum_{m=-(\sqrt{M}-1),m\ odd}^{\sqrt{M}-1}\left[Q\left(\frac{ma - a - \Re\left[(\mathbf{w}_i)^H\mathbf{H}\mathbf{x}_j\right]}{\sqrt{\frac{1}{2}(\mathbf{w}_i)^H\mathbf{C}_n\mathbf{w}_i}}\right) - Q\left(\frac{ma + a - \Re\left[(\mathbf{w}_i)^H\mathbf{H}\mathbf{x}_j\right]}{\sqrt{\frac{1}{2}(\mathbf{w}_i)^H\mathbf{C}_n\mathbf{w}_i}}\right)\right] \tag{15}$$

$$P_{c,i}^{I} = \frac{1}{L_1}\sum_{j=1}^{L_1}\sum_{m=-(\sqrt{M}-1),m\ odd}^{\sqrt{M}-1}\left[Q\left(\frac{ma - a - \Im\left[(\mathbf{w}_i)^H\mathbf{H}\mathbf{x}_j\right]}{\sqrt{\frac{1}{2}(\mathbf{w}_i)^H\mathbf{C}_n\mathbf{w}_i}}\right) - Q\left(\frac{ma + a - \Im\left[(\mathbf{w}_i)^H\mathbf{H}\mathbf{x}_j\right]}{\sqrt{\frac{1}{2}(\mathbf{w}_i)^H\mathbf{C}_n\mathbf{w}_i}}\right)\right] \tag{16}$$

Note: This technique imposes a low computational complexity for the following reasons.

1) Since, we consider the SER only for $m = 0$, the number of computational loops required for calculating the SER will be reduced to M^{N_s-1} from M^{N_s} per iteration.
2) Since, the SER of each constellation point requires a unique representation in terms of the Gaussian error function $Q(\cdot)$, the complexity of calculating all of them is high. However, for our low-complexity solution, we only have to calculate the SER for a single constellation point corresponding to $m = 0$.

The SER of the ith symbol of $\mathbf{x}$ is then formulated for our low-complexity method as

$$\begin{aligned} P_{e,i}^{PSK} &= 1 - \frac{1}{L_2}\sum_{l=1}^{L_2}\int_{-\pi/M}^{\frac{\pi}{M}} p_{\theta,i} d\theta \\ &= \frac{1}{L_2}\sum_{l=1}^{L_2} Q\left[\frac{\mu_{i,l}^R \sin\left(\frac{\pi}{M}\right) - \mu_{i,l}^I \cos\left(\frac{\pi}{M}\right)}{\sigma}\right] \\ &\quad + \frac{1}{L_2}\sum_{l=1}^{L_2} Q\left[\frac{\mu_{i,l}^I \cos\left(\frac{\pi}{M}\right) + \mu_{i,l}^R \sin\left(\frac{\pi}{M}\right)}{\sigma}\right], \end{aligned} \tag{22}$$

where $L_2 = M^{N_s-1}$ and $\mu_{i,l}^R$ or $\mu_{i,l}^I$ represent the values of μ_i^R or μ_i^I (as defined earlier) corresponding to the lth realization of $\mathbf{x}$, respectively.

IV. MBER Based Source-Relay-Destination Link Design

Let us now consider the design of the SRD link based on the MBER CF. This involves a transmit precoder (TPC) matrix design at the SN in addition to the AF matrix of the RN and the equalizer matrix of the DN. We also have to obey the power constraint at the SN involving the TPC matrix in addition to the RN power constraint. The TPC, AF and equalizer matrices are optimized jointly. The CFs are again those of Equations (13), (15), (16), (22), i.e the same as in Section III for various constellations. The optimization problem of the SRD link design can be stated as,

$$\begin{aligned} \mathbf{A}_S^{mber}, \mathbf{A}_F^{mber}, \mathbf{W}_d^{mber} &= \underset{\mathbf{A}_S,\mathbf{A}_F,\mathbf{W}_d}{arg} \min \ P_e(\mathbf{A}_S, \mathbf{A}_F, \mathbf{W}_d) \\ s.t\ (1)\ & Tr\left\{\mathbf{A}_F\left(\sigma_x^2 \mathbf{H}_{sr}\mathbf{H}_{sr}^H + \sigma_r^2 \mathbf{I}_{N_r}\right)\mathbf{A}_F^H\right\} \le P_r \\ (2)\ & \sigma_x^2 Tr\left\{\mathbf{A}_S^H \mathbf{A}_S\right\} \le P_t, \end{aligned} \tag{23}$$

where P_t is the transmit power limit. Additionally, we also consider a suboptimal structure for $\mathbf{A}_S$ for the case of reducing the number of variables during the optimization process. We consider the SVD of $\mathbf{A}_S$ with $\mathbf{A}_S = \mathbf{V}_1\mathbf{\Sigma}_S$, where $\mathbf{V}_1$ is from the SVD decomposition of $\mathbf{H}_{sr}$ and $\mathbf{\Sigma}_S$ is a diagonal matrix having the singular values. We also use the parallel optimization of $P_{e,i}$, as formulated in Section III. With these suboptimal approaches in mind, the optimization problem can be restated as,

$$\begin{aligned} &\text{For i = k :} \\ &\mathbf{\Sigma}_S^{mber}, \mathbf{\Sigma}_F^{mber}, \mathbf{w}_k^{mber} = \underset{\mathbf{\Sigma}_S,\mathbf{\Sigma}_F,\boldsymbol{w}_k}{arg} \min \ P_{e,k}(\mathbf{\Sigma}_S, \mathbf{\Sigma}_F, \mathbf{w}_k) \\ &\qquad s.t\ (1) \sum_{i=1}^{N_r}\sigma_{f,i}^2\left(\sigma_x^2\sigma_{sr,i}^2 + \sigma_r^2\right) \le P_r, \\ &\qquad (2)\ \sigma_x^2\sum_{i=1}^{N_s}\sigma_{s,i}^2 \le P_t. \end{aligned} \tag{24}$$

$$\begin{aligned} &\text{For i} = 1, 2, \ldots, \text{k} - 1, \text{k} + 1, \ldots, N_x : \\ &\mathbf{w}_i^{mber} = \underset{\boldsymbol{w}_i}{arg} \min \ P_{e,i}\left(\mathbf{\Sigma}_S^{mber}, \mathbf{\Sigma}_F^{mber}, \mathbf{w}_i\right), \end{aligned} \tag{25}$$

where $\sigma_{s,i}$ represents the singular value of $\mathbf{A}_S$.

V. Solution of the MBER Optimization Problem

Remarks on CF

The MBER CF may have multiple local minima. As for example, Fig. 2. plots a CF with respect to the equalizer weights (Only the first equalizer $\mathbf{w}_1$) for $N_s = N_r = N_d = 2$ for a fixed real-valued channel and for fixed real-valued $\mathbf{A}_F$ and $\mathbf{A}_S$ matrices for the BPSK signal sets. The equalizer length is 2. For this example, the real-valued channels are assumed to be $\mathbf{H}_{sr} = \begin{bmatrix} -1.12 & 0.74 \\ 0.41 & 0.90 \end{bmatrix}$ and $\mathbf{H}_{rd} = \begin{bmatrix} -1.53 & -0.86 \\ 0.51 & -0.38 \end{bmatrix}$. Observe in Fig. 2 that the CF has several minima with respect to the equalizer weight $\mathbf{w}_1$, hence conventional gradient-based receivers might get stuck in a local optimum, depending on where the search is started on this surface. It is also noted that the solutions obtained from both the MBER and the LMMSE methods are different ((3.4, 8.2) and (5.2, 9.4) for MBER and LMMSE, respectively), while the CF values are 7.8×10^{-3} and 1.1×10^{-2} for MBER and LMMSE methods, respectively. The LMMSE solution might be a reasonable starting point [17].

Binary Genetic Algorithm: Fortunately, random guided optimization methods, like Genetic Algorithms (GA) [21], Simulated Annealing (SA) [24] etc. are capable of circumventing this problem. In this work, we used the binary GA for finding $\mathbf{W}_d$, $\mathbf{A}_F$. As this GA accepts only real-valued variables, we form a vector $\mathbf{v} \in \mathbb{R}^{(N_dN_x+N_rN_s+N_r^2)\times 1}$ by stacking all the real and imaginary components of the $\mathbf{W}_d$, $\mathbf{A}_F$, $\mathbf{A}_S$ matrices as follows

$$\begin{aligned} \mathbf{v} = [&\Re\{vec(\mathbf{W}_d)\}\,\Im\{vec(\mathbf{W}_d)\}\,\Re\{vec(\mathbf{A}_S)\} \\ &\Im\{vec(\mathbf{A}_S)\}\,\Re\{vec(\mathbf{A}_F)\}\,\Im\{vec(\mathbf{A}_F)\}]^T. \end{aligned} \tag{26}$$

Similarly, for the case of the suboptimal scenario, we would form the vector as

$$\mathbf{v} = [\Re\{vec(\mathbf{w}_k)\}\,\{vec(\mathbf{\Sigma}_S)\}\,\{vec(\mathbf{\Sigma}_F)\}]^T. \tag{27}$$

The vector $\mathbf{v}$ is first converted to a binary string and then a series of GA operations like “Parents selection”, “Crossover” and “Mutation” are invoked [21] for finding an improved

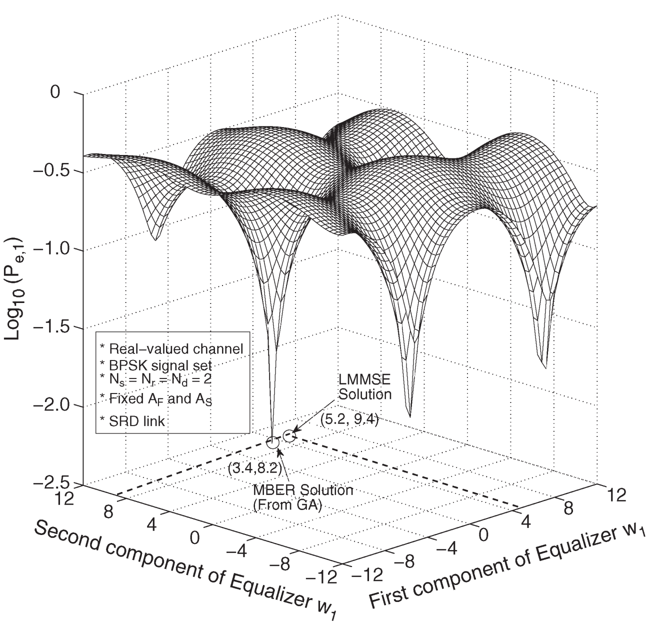

Fig. 2. Logarithm of CF from Equation (11) is plotted with respect to the first equalizer $\mathbf{w}_1$. Equalizer $\mathbf{w}_1$ is real-valued and is of the length 2. $N_s = N_r = N_d = 2$ are associated with fixed $\mathbf{A}_F$ and $\mathbf{A}_S$ matrices and fixed real-valued channel. The signal set is assumed to be BPSK. The MBER solution (obtained from GA) of $\mathbf{w}_1$ is (3.4, 8.2), while its LMMSE solution is (5.2, 9.4). The value of CF at the MBER solution is 7.8×10^{-3}, while it is 1.1×10^{-2} at the LMMSE solution.

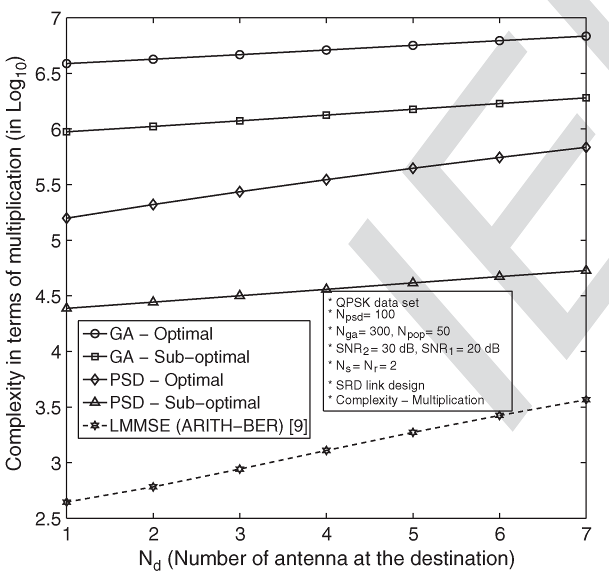

Fig. 3. Complexity (in terms of multiplication) vs. N_d comparison with various optimization options for SRD link design fixing $N_r = 2$, $N_s = 2$, $N_s = N_x$ and QPSK data set.

solution. This binary string is also known as a chromosome. We initially "seed" the GA with an initial solution constituted by the LMMSE one, so that the GA achieves a faster convergence. Unlike any steepest descent method, GA would search through various possible minima using "evolutionary" techniques. Thus, it has a reduced chance of getting into a local minimum compared to the case of completely random initialization. We provide a brief description of the GA in Appendix I. The procedure conceived for finding $\mathbf{A}_F$, $\mathbf{W}_d$ and $\mathbf{A}_S$ with the aid of our constrained binary GA is given in Algorithm. 1.

Algorithm 1: MBER based $\mathbf{A}_F$, $\mathbf{W}_d$ and $\mathbf{A}_F$ design for the relay link (Suboptimal).

1: **Given**: N_s, N_r, N_d, $\mathbf{H}_{sr}$, $\mathbf{H}_{rd}$ with SVD components σ_x^2, σ_r^2, σ_d^2 and P_r along with LMMSE solutions of $\mathbf{W}_d$, $\mathbf{A}_F$ and $\mathbf{A}_S$ as initial "seed".
2: Obtain $\mathbf{\Sigma}_F^{mber}$, $\mathbf{w}_k^{mber}$ from Equation (11) using our constrained binary GA.
3: **for** $i = 1, 2, \ldots, k-1, k+1, \ldots, N_x\}$
4: Substitute $\mathbf{\Sigma}_F^{mber}$ calculated for $i = k$ into $P_{e,i}$.
5: Find $\mathbf{w}_i^{mber}$ from Equation (12) using our binary GA.
6: **end for**
7: **return**$\mathbf{w}_i^{mber}$ for $i = 1, \ldots, N_x$ and $\mathbf{\Sigma}_F^{mber}$, $\mathbf{\Sigma}_S^{mber}$.

Projected Steepest Descent method: We have also used techniques, the low-complexity Projected Steepest Descent (PSD) [22] optimization method, which is one of the steepest descent conceived for constrained optimization [22]. We first form a vector of all the variables of interest. In the case of the optimal scenario, we stack all the complex components of the $\mathbf{W}_d$, $\mathbf{A}_F$ and $\mathbf{A}_S$ matrices to form $\mathbf{v} \in \mathbb{C}^{(N_d N_x + N_r^2 + N_s N_r)\times 1}$ (the variable of interest) as follows

$$\mathbf{v} = \left[\{vec(\mathbf{W}_d)\}\,\{vec(\mathbf{A}_F)\}\,\{vec(\mathbf{A}_S)\}\right]^T. \tag{28}$$

For the PSD method, the updated vector at the jth iteration is obtained as

$$\mathbf{v}_{j+1} = \mathbf{v}_j + \alpha \mathbf{s}_j - \mathbf{G}_j \left(\mathbf{G}_j^H \mathbf{G}_j\right)^{-1} \mathbf{g}_j \tag{29}$$

where $\mathbf{G}_j$ is the gradient of the feasible constraints, $\mathbf{g}_j$ is the stack of feasible constraints and can be defined as follows

$$\mathbf{g}_j = \begin{bmatrix} \left(Tr\left(\mathbf{A}_F\left(\sigma_x^2 \mathbf{H}_{sr}\mathbf{H}_{sr}^H + \sigma_r^2 \mathbf{I}_{N_r}\right)\mathbf{A}_F^H\right) - P_r\right) \\ \left(\sigma_x^2\left(Tr\left(\mathbf{A}_S^H \mathbf{A}_S\right)\right) - P_t\right) \end{bmatrix} \tag{30}$$

We also define $\mathbf{s}_j$ as follows

$$\mathbf{s}_j = -\left[\mathbf{I} - \mathbf{G}_j\left(\mathbf{G}_j^H \mathbf{G}_j\right)^{-1}\mathbf{G}_j^H\right]\nabla f(\mathbf{x}_j). \tag{31}$$

along with $\alpha = -(\gamma f(\mathbf{x}_j)/\mathbf{s}_j^H \nabla f(\mathbf{x}_j))$, where γ is the desired reduction factor, usually assumed to be 0.05 (5%). For our specific problem with the optimal case, $\mathbf{G}_j$ will be obtained as follows

$$\mathbf{G}_j = \begin{bmatrix} vec\left(\mathbf{0}_{N_d \times N_x}\right) & vec\left(\mathbf{0}_{N_d \times N_x}\right) \\ vec\left(\mathbf{A}_F \mathbf{A}_1\right) & vec\left(\mathbf{0}_{N_r \times N_r}\right) \\ vec\left(\mathbf{0}_{N_s \times N_s}\right) & vec\left(\mathbf{A}_S\right) \end{bmatrix} \tag{32}$$

where $\mathbf{A}_1 \triangleq (\sigma_x^2 \mathbf{H}_{sr}\mathbf{H}_{sr}^H + \sigma_r^2 \mathbf{I}_{N_r})(\sigma_x^2 \mathbf{H}_{sr}\mathbf{H}_{sr}^H + \sigma_r^2 \mathbf{I}_{N_r})^H$. For the suboptimal case, $\mathbf{G}_j$ would be obtained as follows

$$\mathbf{G}_j^{sub} = \begin{bmatrix} vec\left(\mathbf{0}_{N_d \times 1}\right) & vec\left(\mathbf{0}_{N_d \times 1}\right) \\ \mathbf{c}_1 & vec\left(\mathbf{0}_{N_r \times 1}\right) \\ vec\left(\mathbf{0}_{N_x \times 1}\right) & \mathbf{c}_2 \end{bmatrix} \tag{33}$$

TABLE II
COMPUTATION COMPLEXITY COMPARISON BETWEEN THE PROPOSED MBER METHOD WITH LMMSE METHOD FOR SRD RELAY

Algorithm	MBER Complexity
GA (Multiplication) (Optimal)	$N_{pop}N_{ga}(4N_rN_d(N_r+N_s) +4N_rN_sN_x+4N_dN_r^2+2N_d^2 +N_x(4N_d^2+4N_d)+4N_dN_sN_x+8N_r^3 +2N_xM^{N_x}(4N_x+1+N_Q)+4N_r^2N_s +2N_r^2+4N_s^2N_x+1)$
GA (Total operations) (Optimal)	$N_{pop}N_{ga}(2N_d(N_r+N_s)(4N_r-1) +(8N_s-2)N_rN_x+(8N_r-2)N_rN_d +2N_d^2+N_d+N_x(8N_d^2+6N_d-2) +4N_dN_sN_x+2N_xM^{N_x}(4N_x+1+N_Q) +N_r^2(8N_s+16N_r-6)+2N_r +2(N_r-1)+(8N_s-2)N_sN_x-1$
GA (Multiplication) (Sub-optimal)	$N_{pop}N_{ga}(3\min(N_d,N_r,N_s,N_x) +2N_dN_x+4N_dN_r^2+2N_d^2 +N_x+N_x(4N_d^2+4N_d)+4N_dN_sN_x +2N_xM^{N_x}N_Q+2N_r+1)$
GA (Total operations) (Sub-optimal)	$N_{pop}N_{ga}(3\min(N_d,N_r,N_s,N_x) +2N_dN_x+(8N_r-2)N_rN_d+2N_d^2 +N_x(8N_d^2+6N_d-2)+4N_dN_sN_x +2N_xM^{N_x}N_Q+3N_r+N_s+1+N_d)$

where $[\mathbf{c}_1]_i = (\sigma_x^2\sigma_{sr,i}^2 + \sigma_r^2)$ and $[\mathbf{c}_2]_i = \sigma_x^2$. For suboptimal case, $\mathbf{g}_j$ is defined as follows

$$\mathbf{g}_j^{sub} = \begin{bmatrix} \left(\sum_{i=1}^{N_r} \sigma_{f,i}^2(\sigma_x^2\sigma_{sr,i}^2+\sigma_r^2) - P_r\right) \\ \left(\sigma_x^2 \sum_{i=1}^{N_s} \sigma_{s,i}^2 - P_t\right) \end{bmatrix} \tag{34}$$

For all cases, the initial value of $\mathbf{v}$ is chosen from the LMMSE solution.

VI. COMPUTATIONAL COMPLEXITY ANALYSIS

Let us now approximate the computational complexity of the relay link designs using the MBER CF. We express it in terms of the number of operations, which can be addition, subtraction and multiplication operations. We first quantify the complexity in terms of the number of multiplications and then in terms of all the operations. We found that the complexity is dominated by the multiplications due to the associated matrix operations. We have also considered the complexity separately for both the optimal and sub-optimal approaches. Let us assume that N_{pop} and N_{ga} are the population size and the average number of GA iterations, respectively. The complexity results are presented in Table II for the SRD case. However, the details of the analysis are given in Appendix II along with the RD case as well. We have also analyzed the detailed complexity involving the PSD optimization, albeit they are not given in the table due to space limitations.

Notes:

1) An approximation for N_Q can be obtained in several ways. In practice, the $Q(\cdot)$-function is calculated using the look-up table. Ignoring the off-line calculations of its values at various data points, we need to compute the index of the discretized argument, which needs one unit of operation followed by a memory-read. The other approach is constituted by the more accurate Taylor series.

$$Q(x) = \frac{1}{2} - \frac{1}{\sqrt{2\pi}} \sum_{n=0}^{\infty} \frac{(-1)^{(n)} x^{2n+1}}{n!(2n+1)2^n}. \tag{35}$$

We note that typically $2n$ is calculated by the left-shifting of the binary string by one position and 2^n is simply a binary number of length $(n+1)$ with only a single '1' at the $(n+1)^{th}$ position. Thus, we can ignore the complexity involving these two operations. Now, we can calculate the N_Q as $N_Q \approx 4N_{lim}$ with multiplications and $N_Q \approx 5N_{lim}$ with total operations, respectively, where N_{lim} is a number for representing the limit of Taylor series sum. Simulation shows that even $N_{lim} \geq 20$ gives a good approximation with argument $x \leq 4$.

2) In the complexity analysis, another complexity component involving the SVD decomposition of a matrix has to be mentioned, which is required for both the LMMSE algorithm and for our proposed low complexity solution. For the channel matrices $\mathbf{H}_{sr}$ and $\mathbf{H}_{rd}$, the order of complexity will be $O(4N_r^2N_s+22N_s^3)+O(4N_d^2N_r+22N_r^3)$.

3) The computational complexity of the LMMSE solution relying on ARITH-BER [9] has not been analyzed in [9], hence we analyze it for comparison. The complexity in terms of the multiplications is approximately $4N_s^2N_x + 8N_s + 4 + 19N_s + 2N_r + 4N_r^3 + 4N_r\, N_s^2 + (32N_s^3 - 12N_s^2 - 2N_s)/6 + 3\min(N_d, N_s, N_r, N_x) + 2N_dN_x + (32N_d^3 - 12N_d^2 - 2N_d)/6 + 4N_dN_r^2 + 2N_d^2 + 4N_dN_sN_x + 4N_sN_d^2 + 2N_sN_d$. The total complexity is approximately $(8N_s-2)N_sN_x + 29N_s + 3 + (8N_r-2)N_r^2 + 2N_r + (8N_s-2)N_rN_s + (32N_s^3 + 60N_s^2 - 14N_s)/3 + (8N_s - 2)N_dN_x + (8N_d-2)N_sN_d + 2N_sN_d + 4N_d^2 + (32N_d^3 + 60\,N_d^2 - 14\,N_d)/3 + 3\min(N_d,N_r,N_s,N_x)\,2N_d\,N_x + (8N_r-2)N_rN_d + N_d$.

VII. NUMERICAL RESULTS

Let us now study the BER performance of the proposed method against that of the LMMSE method [7]. Our simulations are performed in two stages. During the first stage, we use a known training sequence for determining both the TPC as well as the AF and equalizer matrices of the SN, RN, DN respectively. In the second stage, the data sequence is detected. We consider a flat Rayleigh fading i.i.d channel with unit variance for each complex element of $\mathbf{H}_{sr}$ and $\mathbf{H}_{rd}$. Thus, the Channel Impulse Response (CIR) is a non-dispersive Rayleigh-faded one. Most of the simulations are preformed for $N_s = 2$, $N_r = 2$, $N_d = 2$ with channel coding, which uses Convolution Code (CC) of $(7,5)_8$. We have used the Soft-Output Viterbi decoding [23]. The RN's SNR is defined as $\mathrm{SNR}_1 = 10\log_{10}((\sigma_x^2/\sigma_1^2))$ dB, where σ_x^2 is the power of each x_i, which is set to (P_t/N_x) with $P_t = 1$ dBm. The DN's SNR is defined as $\mathrm{SNR}_2 = 10\log_{10}((P_r/N_r\sigma_2^2))$ dB, with the RN power constraint of $P_r = 5$ dBm. Finally the SN's power is constrained to $P_t = 1$ dBm unless specified otherwise. The SNR_1 is kept at 20 dB. Our simulation results are averaged

TABLE III
GA PARAMETERS

Parameters	*Values*
Population Size	50
GA maximum iteration limit	500
Mutation Type	Bit flipping
Probability of mutation	0.01
Binary string length per variable	16 bit
Initialization	LMMSE
Crossover type	Single point

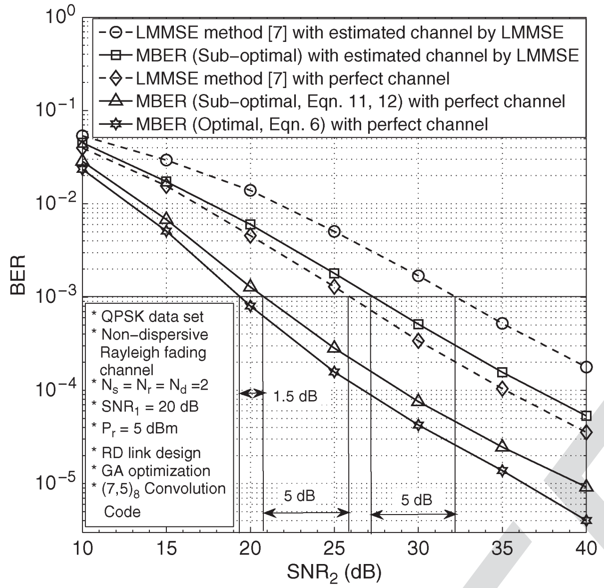

Fig. 4. BER vs. SNR_2 performance of the RN-DN link design based on the MBER method (with full $\mathbf{A}_F$, $\mathbf{W}_d$ (equation (6)) and suboptimal methods (equations (11) and (12)) along with the LMMSE method over a flat Rayleigh fading channel. Performances with and without the channel estimation are presented. $N_s, N_r, N_d = 2$, P_r is constrained to 5 dBm and SNR_1 is 20 dB. Convolution code of $(7,5)_8$ is used along with the GA optimization.

over 1000 channel realizations per SNR value. In all our simulation setup, we have assumed $N_x = N_s$, though any value of N_x can be assumed. The GA related parameters are chosen as per Table III.

Experiment 1: This experiment is for the RD link design. The primary focus of this experiment is to characterize the BER performance of the proposed MBER method against that of the LMMSE benchmark [7]. We have also evaluated the BER performance both with perfect and with estimated channel, where the channel was also estimated using the LMMSE technique. In the second part of the experiment, we characterized the various suboptimal methods along with the original problem formulation of Equation (6) for analyzing the effects of $\mathbf{A}_F$ and $\mathbf{W}_d$. In this experiment, we have also shown the superiority of the MBER method over a rank-deficient system, where conventional LMMSE technique fails to perform adequately. *Remarks*:

1) Fig. 4. plots the BER vs. SNR_2 performance of both the MBER and LMMSE based RD link design. Observe in Fig. 4 that as the SNR increases, the MBER method increasingly outperforms the LMMSE method.

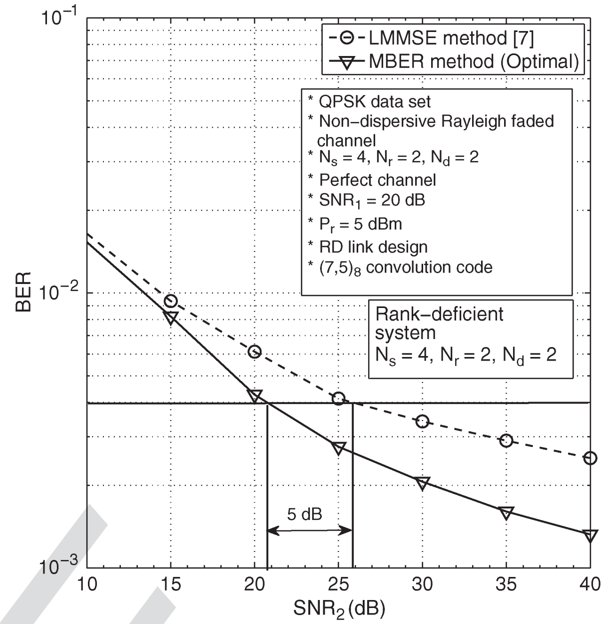

Fig. 5. BER vs. SNR_2 performance of the rank-deficient RN-DN link design based on the MBER method (optimal) along with the LMMSE method over a flat Rayleigh fading perfect channel. $N_s = 4$ and $N_r, N_d = 2$, P_r is constrained to 5 dBm and SNR_1 is 20 dB. Convolution code of $(7,5)_8$ is used along with the GA optimization.

At $\mathrm{BER} = 10^{-3}$ the MBER method requires an SNR of approximately 19.5 dB (suboptimal, SVD based) and 20.7 dB (optimal), respectively, while the LMMSE method needs SNR ≈ 26 dB for the perfectly known channel. Thus, the MBER method attains an SNR gain of approximately 5 dB (suboptimal) and 6.5 dB (optimal), respectively for the scenario of $\mathrm{SNR}_1 = 20$ dB and $P_r = 5$ dBm. The SNR gain of the LMMSE-estimated channel remains almost ≥ 5 dB for the suboptimal MBER based RN-DN link design.

2) Fig. 5 shows the BER performance of a rank-deficient system. The $N_s = 4$ with $N_r = 2N_d = 2$. It shows that at $\mathrm{BER} = 4 \times 10^{-3}$, the MBER method gives a BER gain of almost 5 dB, where conventional LMMSE method fails to perform adequately.

3) Let us now consider both the SVD structure of $\mathbf{A}_F$ and its original non-decomposed structure. In both the cases, we generate $\mathbf{w}_i$ in both ways, first as in Equation (6) and then as in Equations (11) and (12). Fig. 6 characterizes all these cases. Observe that at $\mathrm{BER} = 10^{-3}$, the SVD structure based $\mathbf{A}_F$ obtains a degraded SNR performance of 1.5 dB compared to the case, where $\mathbf{A}_F$ assumes no SVD structure. It is also observed from Fig. 6 that the two choices for determining the equalizer matrix $\mathbf{W}_d$ do not have severe impact on the performance. This implies that $\mathbf{A}_F$ dominates the CF compared to the equalizer matrix $\mathbf{W}_d$ in the MBER framework. This also highlights the fact that our low-complexity solution of Equations (11) and (12) conceived for determining the DN's equalizers in parallel does not impose any substantial degradation on the BER performance in Fig. 6.

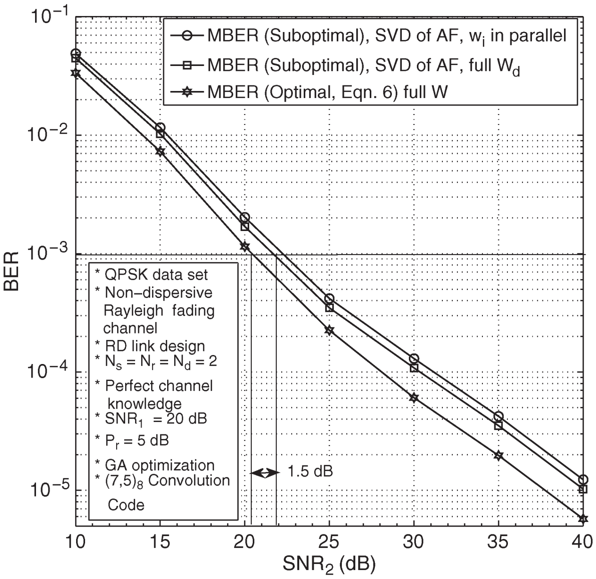

Fig. 6. BER vs. SNR_2 performance of the RD link design based on the MBER method with various options for $\mathbf{A}_F$ and $\mathbf{W}_d$ matrices (Various combinations of equations (6) and (11), (12)) with a flat Rayleigh fading channel. Channels are perfectly known. $N_s, N_r, N_d = 2$, P_r is constrained to 5 dBm and SNR_1 is 20 dB with CC code of $(7, 5)_8$.

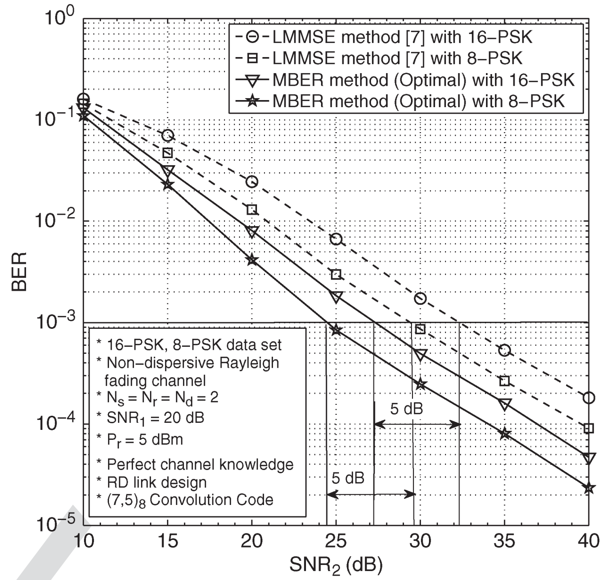

Fig. 7. BER vs. SNR_2 performance of the RD link design based on the MBER method over a flat Rayleigh fading channel with 8- and 16-PSK signal sets with CC code of $(7, 5)_8$. Channels are perfectly known. $N_s, N_r, N_d = 2$ with P_r and SNR_1 being constrained to 5 dBm and 20 dB, respectively.

Experiment 2: Thi experiment characterizes the BER performance of both 8-PSK and 16-PSK relying on the MBER CF for transmission over a flat Rayleigh fading channel for the RD link. The channels are assumed to be perfectly known. The rest of the experimental setup is the same as in Experiment-1. *Remarks*:

1) Fig. 7 plots the BER of the MBER method for both 8-PSK and 16-PSK. Observe in Fig. 7 that at the BER = 10^{-3} 8-PSK using the MBER CF requires an SNR of approximately 24.5 dB (suboptimal, SVD), while the LMMSE method needs approximately 29.5 dB. Thus, the MBER method provides an SNR gain of approximately 5 dB (suboptimal) in conjunction with $\mathrm{SNR}_1 = 20$ dB and $P_r = 5$ dBm for 8-PSK. Similar BER improvements are attained also for 16-PSK.

Experiment 3: In this experiment, the Gaussian $Q(\cdot)$-function encapsulated in the CF is approximated by the less complex function of $Q(x) \approx (1/2)e^{-x^2/2}$[23]. In Fig. 8, we only characterize the RD link, this investigation may be readily extended to the SRD link design as well. Again, the channels are assumed to be perfectly known in this experiment. *Remarks*:

1) Fig. 8 portrays the BER performance of the MBER method using the above-mentioned $Q(x) \approx (1/2)e^{-x^2/2}$ approximation for the RD link, which reduces the complexity of the search from that of Equation (11) to Equation (12) imposed, when finding $\mathbf{A}_F$ and $\mathbf{W}_d$. Observe in Fig. 8 that the performance penalty imposed by this approximation is negligible at higher SNR values (> 25 dB), although at lower SNR values this degradation is non-negligible.

Experiment 4: In this experiment we consider the SRD link using our proposed MBER based framework. We have also

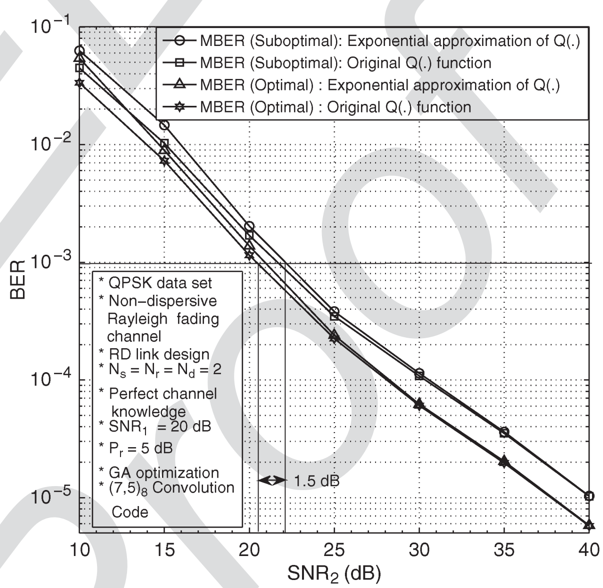

Fig. 8. BER vs. SNR_2 performance of the RD link design based on the MBER method with the Gaussian error function $Q(.)$-function approximation to an exponential one over a flat Rayleigh fading channel. Channels are perfectly known. QPSK signal set is used with CC code of $(7, 5)_8$. $N_s, N_r, N_d = 2$ with P_r being constrained to 5 dBm.

considered a $4 \times 2 \times 2$ rank-deficient SRD case. We set the SN and RN power constraints to be $P_t = 5$ dBm and $P_r = 5$ dBm, respectively. We do not invoke the SVD of the $\mathbf{A}_F$ and $\mathbf{A}_S$ matrices in this experiment. The channels are assumed to be perfectly known. We have used CC code of $(7, 5)_8$. In this experiment, we have used both GA with LMMSE "seed" and PSD with LMMSE initial solution. *Remarks*:

1) Fig. 9 characterizes the BER performance of the SN-RN-DN link using our MBER framework. With GA method, at the BER = 10^{-3}, the MBER method requires an SNR

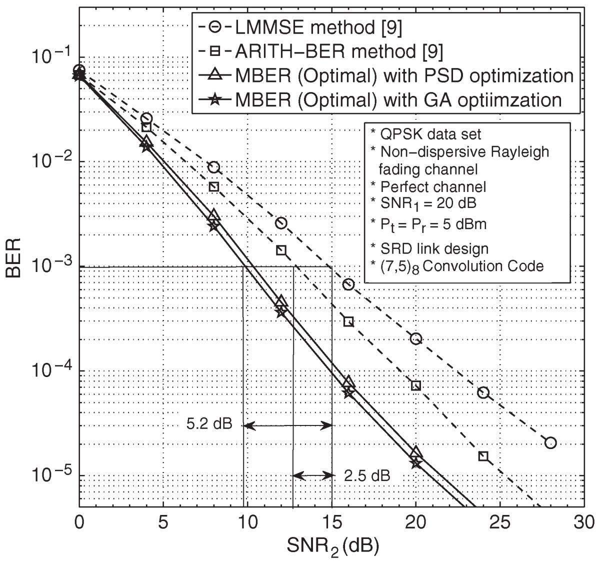

Fig. 9. BER vs. SNR_2 performance of the SRD link design based on the MBER method over a flat Rayleigh fading channel. Channels are perfectly known. $N_s, N_r, N_d = 2$, P_r and P_t are constrained to 5 dBm and SNR_1 is 20 dB. QPSK signal set is used with CC code of $(7,5)_8$. GA and PSD optimizations are used.

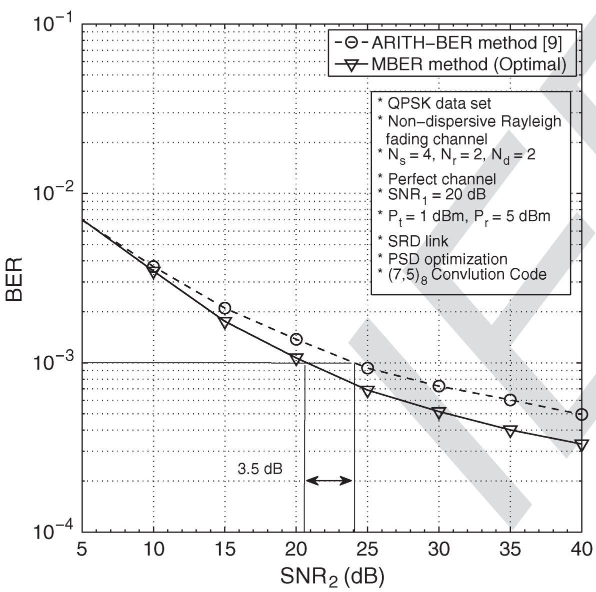

Fig. 10. BER vs. SNR_2 performance of a rank-deficient $4 \times 2 \times 2$ SRD link design based on the MBER method over a flat Rayleigh fading channel. Channels are perfectly known. $N_s = 4$, $N_r, N_d = 2$, P_r and P_t are constrained to 5 dBm and SNR_1 is 20 dB. QPSK signal set is used with CC code of $(7,5)_8$. PSD optimization is used.

of approximately 9.8 dB (optimal), while the LMMSE method needs 15 dB and ARITH-BER requires 13.5 dB, respectively. Thus, the MBER method attains an SNR gain of approximately 5.2 dB and 3.7 dB for the SRD link with respect to LMMSE and ARITH-BER, respectively. We observe that PSD gives a 0.7 dB SNR degradation.

2) Fig. 10 shows the BER performance of the rank-deficient case. It shows that we can still attain an SNR gain of almost 3.5 db at the BER $= 1 \times 10^{-3}$ with coded data along with the PSD optimization method.

VIII. Conclusions

New MBER-based TPC, AF and equalizer matrices were designed for the RN-DN link and SN-RN-DN links. The CFs of various constellations were derived and a solution was found for the design of these matrices using the MBER framework. Sub-optimal approaches have also been proposed for computational complexity reduction. It was shown that the BER performance of the proposed method is superior compared to the LMMSE method, albeit this improved performance has been achieved at an increased computational complexity.

Appendix I
Optimization Techniques

In this contribution, we have adopted two optimization methods, namely the binary GA [21] and the PSD [22]. Below we provide a brief description of the GA technique in the context of our problem.

A. Binary GA

The binary GA is a heuristic method of optimization [21]. We form a vector also referred to as a chromosome from the variables of interest by stacking all the variables' real and imaginary components as defined in Equation (26).

1) *Population selection* GA commences its operation from a set of initial chromosome values known as the initial population having a size of N_{pop}. The initial solution can be randomly generated or "seeded" with a better initial choice. The second option leads to a faster convergence. In our case, the "seed" is the "LMMSE" solution and the initial population is generated with the aid of a slight random variation around the "seed". Now, for every chromosome in the population, a "fitness" value is obtained by calculating the CF value against each of them. Then, the Roulette-Wheel algorithm of [21] is invoked for selecting the suitable parent solutions for generating child solutions for the next iteration. A pair of techniques referred to as crossover and mutation are invoked for generating children from the parents.
2) *Crossover* The crossover operation is a chromosome "reproduction" technique by which an off-spring is generated upon picking various parts of its parent chromosome. This method introduces a large amount of characteristic variation into the off-spring. Let us consider the following example. Let us assume that a random binary string, $B1$, which has the same length as chromosome is created. We also assume that two children, namely $Ch1$ and $Ch2$ have to be created from two parent chromosomes $P1$ and $P2$. Then, if the ith position of $B1$ is 0, $Ch1$ and $Ch2$ would fill up their ith position from the ith position of $P1$ and $P2$, respectively. Otherwise, the ith position of $P1$ would populate $Ch2$ and that of $P2$ would go to $Ch1$.

$$P1 = [11000110];$$
$$P2 = [10111001];$$
$$B1 = [00101011]; \tag{36}$$

Hence, the children become

$$Ch1 = [11101101];$$
$$Ch2 = [10010010]; \tag{37}$$

Mutation Mutation is a relatively small-scale characteristic variational "reproduction" tool for off-spring generation. It introduces a bit flipping at a few randomly selected places of the chromosomes. For example, if a parent chromosome is $P = [11000110]$, a mutation at the 2nd Least-Significant-Bit (LSB) position generates a child $Ch = [11000100]$.

3) *Termination* Using the crossover and mutation techniques, a new set of off-spring is generated along with their fitness value. If one of them satisfies the required fitness value, the process is terminated with that chromosome being the solution. The process is also terminated, if the maximum number of iterations is exceeded. If no sufficiently good fit is found at a given iteration (provided the maximum iteration number has not been reached), the algorithm goes ahead with the selection of parents from the current set of children using the Roulette-Wheel algorithm mentioned earlier.

Appendix II
Detail Complexity Analysis

The CF of BPSK formulated in Equation (13) is considered here first for this calculation, which is readily extended to other constellations as well. However, it is noted that the overall complexity depends on the specific choice of optimization method. We first calculate the complexity of calculating the CF and constraints once, irrespective of the choice of optimization method.

RN-DN Link: Let us commence with the BPSK CF Equation (13). Let us first consider the term $(\mathbf{w}_i)^H\mathbf{H}\mathbf{x}_j x_i$. The fundamental assumption is that multiplication of two complex numbers would take 4 real data multiplication and 6 total operation (2 extra additions are required). Hence, two complex matrices of orders $\mathbb{C}^{M\times N}$ and $\mathbb{C}^{N\times K}$ would take $4MNK$ multiplications, whereas the total operation required is $(8N-2)MK$. Multiplication of a complex-valued matrix and a vector of order $\mathbb{C}^{M\times N}$ and $\mathbb{C}^{N\times 1}$ would require $4MN$ multiplications and $(8N-2)M$ total operations, respectively.

1) Thus, effective channel matrix $\mathbf{H}$ takes $N_1^m = 4N_rN_d(N_r+N_s)$ multiplications and $N_1^t = 2N_d(N_r+N_s)(4N_r-1)$ total operations respectively. Calculation of $\mathbf{H}$ is common with all the equalizers $\mathbf{w}_i$.
2) $(\mathbf{w}_i)^H\mathbf{H}\mathbf{x}_j x_i$ requires $N_2^m = 4N_dN_s + 4N_s + 1$ multiplications and $N_2^t = 8N_sN_d + 6N_d - 1$ total operations, respectively.
3) Similarly, the noise covariance matrix $\mathbf{C}_n$(4) requires $N_3^m = 4N_dN_r^2 + 2N_d^2$ multiplications and $N_3^t = (8N_r-2)N_rN_d + 2N_d^2 + N_d$ total operations, respectively. It assumes that calculation of $\mathbf{H}_{rd}\mathbf{A}_F$ is already done with $\mathbf{H}$. Calculation of $\mathbf{C}_n$ is common with all the equalizers $\mathbf{w}_i$.
4) Thus, $\mathbf{w}_i^H\mathbf{C}_n\mathbf{w}_i$ requires $N_4^m = 4N_d^2 + 4N_d$ multiplication and $N_4^t = 8N_d^2 + 6N_d - 2$ total operations, respectively.
5) Assuming the square root and division as two unit of operations, the total complexity of calculating the CF once is $N_5^m = N_1^m + N_3^m + N_xN_4^m + 4N_dN_sN_x + N_x2^{N_x}(4N_x+1+N_Q)$ (with only multiplication) and $N_5^t = N_1^m + N_3^m + N_xN_4^t + Nx(8N_sN_d - 2Ns) + 2^{N_x}(8N_x + 1 + N_Q)$ (with total operations), respectively, where N_Q is the complexity involving the $Q(\cdot)$-function.
6) If M-QAM is chosen, the complexity will be approximately $N_5^m \approx N_1^m + N_3^m + N_xN_4^m + 4N_dN_sN_x + 2N_xM^{N_x}(4N_x + 1 + N_Q)$ with multiplication and $N_5^t \approx N_1^t + N_3^t + N_xN_4^t + 6N_s^2N_d + 2N_xM^{N_x}(2N_xN_d + 6N_d + N_Q)$ with the total complexity, respectively. For the M-PSK case with the rotated constellation concept, we need to multiply $(4N_x+1+N_Q)$ with only $2N_xM^{N_x-1}(4N_x+1+N_Q)$.
7) For the SVD-based approach, the complexity of $\mathbf{H}$ requires $N_1^m = \min(N_d, N_r) + 2N_d^2 + 4N_dN_s^2$ multiplications and $N_1^t = \min(N_d, N_r) + 2N_d^2 + (8N_s - 2)N_dN_s$ total operations.
8) Let us calculate the complexity involving the constraints. From equation (6), we obtain the complexity for constraints as $N_1^{m,c} = 8N_r^3 + 4N_r^2N_s + 2N_r^2$ with multiplication only and $N_1^{t,c} = N_r^2(8N_s + 16N_r - 6) + 2N_r + 2(N_r - 1)$ with total operations, respectively. For the SVD approach, it would be $N_1^{m,c} = 2N_r$ with multiplications and $N_1^{t,c} = 3N_r$ total operations, respectively.

SN-RN-DN Link: For the case of the SN-RN-DN link, we have to additionally incorporate the calculation of the TPC matrix $\mathbf{A}_S$.

1) We obtain the complexity for $\mathbf{H}$ as $N_1^m = 4N_rN_d(N_r + N_s) + 4N_rN_sN_x$ with multiplication and $N_1^t = 2N_d(N_r+N_s)(4N_r-1) + (8N_s-2)N_rN_x$ with total operations, respectively. For the SVD-based approach, we obtain $N_1^m = 3\min(N_d, N_r, N_s, N_x) + 2N_dN_x$ for multiplications and $N_1^t = N_1^m$ as well for the total operations.
2) An additional complexity for the source power constraint may be calculated as $N_2^{m,c} = 4N_s^2N_x + 1$ with multiplication and $N_2^{t,c} = (8N_s-2)N_sN_x + 2N_s - 1$ with total computations, respectively. For the SVD-based approach, they become $N_2^{m,c} = 1$ for multiplication and $N_2^{t,c} = N_s + 1$ for total operations, respectively.

Computational-Complexity, Specific to Optimization Method: Computational complexity is also dependent on the specific choice of optimization algorithm to determine the parameters. For binary GA, time-complexity is more appropriate. However, we try to give an approximate computational-complexity for GA. The computational-complexity for GA is dominated by the function and constraint evaluations to determine the eligible population at each iterations. Let us assume that total size of population is N_{pop} and GA requires N_{ga} iterations to converge. Then, total complexity will be approximately $N_{pop}N_{ga}(N_5^m + N_1^{m,c} + N_2^{m,c})$ with multiplication and $N_{pop}N_{ga}(N_5^t + N_1^{t,c} + N_2^{t,c})$ with total operations, respectively.

For the PSD algorithm, we need to calculate the gradient for both function and constraint. Gradient of CF is calculated numerically.

1) Gradient of CF takes $N_1^{m,psd} = 2(N_d N_x + N_r^2 + N_s N_r) N_5^m$ multiplication and $N_1^{t,psd} = 2(N_d N_x + N_r^2 + N_s N_r) N_5^t$ total operations, if we use numerical method. For the SVD-based approach, it would be $N_1^{m,psd} = 2(N_d + N_x + N_r) N_5^m$ with multiplication and $N_1^{t,psd} = 2(N_d + N_x + N_r) N_5^t$ with total operations.
2) Per iteration, other steps require $N_2^{m,psd} = 18(N_r^2 + N_s N_r) + 6(N_d N_x + N_r^2 + N_s N_r) + 4(N_r^2 + N_s^2)^2 + 9$ multiplications and $N_2^{t,psd} = 25(N_r^2 + N_s N_r) + 22 + 10(N_d N_x + N_r^2 + N_s N_r) + 8(N_r^2 + N_s N_r)^2$ total operations. For sub-optimal case, it would be $N_2^{m,psd} = 2(N_r^2 + N_s^2) + 3(N_d + N_r + N_s) + 1 + 2(N_d + N_s)$ for multiplication and $N_2^{t,psd} = 6(N_r + N_s) - 6 + 7(N_d + N_r + N_s)$ for total operations.
3) If PSD takes an average iteration of N_{psd}, the computational complexity may be approximated as $N_{psd}(N_1^{m,psd} + N_2^{m,psd})$ with multiplication and $N_{psd}(N_1^{t,psd} + N_2^{t,psd})$ with total operations.

Computational Complexity for LMMSE [9]-ARITH BER Case: We give an approximate computational complexity for the LMMSE case for comparison purpose.

1) The computation of precoder matrix $\mathbf{A}_S$ requires $4N_s^2 N_x + 8N_s + 3$ multiplication and $(8N_s - 2)N_s N_x + 5N_s + 1$ total operations.
2) The computation of AF matrix requires $19N_s + 1 + 2N_r + 4N_r^3 + 4N_r N_s^2 + (32N_s^3 - 12N_s^2 - 2N_s)/6$ multiplications and $24N_s + 2 + (8N_r - 2)N_r^2 + 2N_r + (8N_s - 2)N_r N_s + (32N_s^3 + 60N_s^2 - 14N_s)/3$ total operations.
3) Computation of effective channel matrix and noise covariance matrix are already given.
4) Computation of equalizer matrix requires $4N_d N_s N_x + 4N_s N_d^2 + 2N_s N_d + (32N_d^3 - 12N_d^2 - 2N_d)/6$ multiplications and $(8N_s - 2)N_d N_x + (8N_d - 2)N_s N_d + 2N_s N_d + 2N_d^2 + (32N_d^3 + 60N_d^2 - 14N_d)/3$ total operations.

ACKNOWLEDGMENT

The financial support of the DST, India and of the EPSRC, UK under the auspices of the India-UK Advanced Technology Centre (IUATC) is gratefully acknowledged.

REFERENCES

[1] Y. Rong, X. Tang, and Y. Hua, "A unified framework for optimizing linear nonregenerative multicarrier MIMO relay communication systems," *IEEE Trans. Signal Process.*, vol. 57, no. 12, pp. 4837–4851, Dec. 2009.
[2] Y. Rong, "Optimal linear non-regenerative multi-hop MIMO relays with MMSE-DFE receiver at the destination," *IEEE Trans. Wireless Commun.*, vol. 9, no. 7, pp. 2268–2279, Jul. 2010.
[3] X. J. Zhang and Y. Gong, "Adaptive power allocation for multihop regenerative relaying with limited feedback," *IEEE Trans. Veh. Technol.*, vol. 58, no. 7, pp. 3862–3867, Sep. 2009.
[4] X. J. Zhang and Y. Gong, "Jointly optimizing power allocation and relay positions for multi-relay regenerative relaying with relay selection," in *Proc. 4th ICSPCS*, 2010, pp. 1–9.
[5] J. Zou, H. Luo, M. Tao, and R. Wang, "Joint source and relay optimization for non-regenerative MIMO two-way relay systems with imperfect CSI," *IEEE Trans. Wireless Commun.*, vol. 11, no. 9, pp. 3305–3315, Sep. 2012.
[6] W. Zhang, U. Mitra, and M. Chiang, "Optimization of amplify-and- forward multicarrier two-hop transmission," *IEEE Trans. Commun.*, vol. 59, no. 5, pp. 1434–1445, May 2011.
[7] W. Guan and H. Luo, "Joint MMSE transceiver design in non- regenerative MIMO relay systems," *IEEE Commun. Lett.*, vol. 12, no. 7, pp. 517–519, Jul. 2008.
[8] C. Jeong and H.-M. Kim, "Precoder design of non-regenerative relays with covariance feedback," *IEEE Commun. Lett.*, vol. 13, no. 12, pp. 920–922, Dec. 2009.
[9] C. Song, K.-J. Lee, and I. Lee, "MMSE based transceiver designs in closed-loop non-regenerative MIMO relaying systems," *IEEE Trans. Wireless Commun.*, vol. 9, no. 7, pp. 2310–2319, Jul. 2010.
[10] C. Xing, S. Ma, and Y.-C. Wu, "Robust joint design of linear relay precoder and destination equalizer for dual-hop amplifyand- forward MIMO relay systems," *IEEE Trans. Signal Process.*, vol. 58, no. 4, pp. 2273–2283, Apr. 2010.
[11] X. Tang and Y. Hua, "Optimal design of non-regenerative MIMO wireless relays," *IEEE Trans. Wireless Commun.*, vol. 6, no. 4, pp. 1398–1407, Apr. 2007.
[12] O. Munoz-Medina, J. Vidal, and A. Agustin, "Linear transceiver design in nonregenerative relays with channel state information," *IEEE Trans. Signal Process.*, vol. 55, no. 6, pp. 2593–2604, Jun. 2007.
[13] B. Sainath and N. Mehta, "Generalizing the amplify-and-forward relay gain model: An optimal SEP perspective," *IEEE Trans. Wireless Commun.*, vol. 11, no. 11, pp. 4118–4127, Nov. 2012.
[14] T. Peng, R. de Lamare, and A. Schmeink, "Joint minimum BER power allocation and receiver design for distributed space-time coded cooperative MIMO relaying systems," in *Proc. Int. ITG WSA*, 2012, pp. 225–229.
[15] C.-C. Yeh and J. Barry, "Adaptive minimum bit-error rate equalization for binary signaling," *IEEE Trans. Commun.*, vol. 48, no. 7, pp. 1226–1235, Jul. 2000.
[16] W. Yao, S. Chen, and L. Hanzo, "Generalised vector precoding design based on the MBER criterion for multiuser transmission," in *Proc. IEEE VTC-Fall*, 2010, pp. 1–5.
[17] S. Chen, A. Livingstone, and L. Hanzo, "Minimum bit-error rate design for space-time equalization-based multiuser detection," *IEEE Trans. Commun*, vol. 54, no. 5, pp. 824–832, May 2006.
[18] W. Yao, S. Chen, and L. Hanzo, "Generalized MBER-based vector precoding design for multiuser transmission," *IEEE Trans. Veh. Technol.*, vol. 60, no. 2, pp. 739–745, Feb. 2011.
[19] W. Yao, S. Chen, and L. Hanzo, "A transceiver design based on uniform channel decomposition and MBER vector perturbation," *IEEE Trans. Veh. Technol.*, vol. 59, no. 6, pp. 3153–3159, Jul. 2010.
[20] M. Alias, S. Chen, and L. Hanzo, "Multiple-antenna-aided OFDM employing genetic-algorithm-assisted minimum bit error rate multiuser detection," *IEEE Trans. Veh. Technol.*, vol. 54, no. 5, pp. 1713–1721, Sep. 2005.
[21] D. E. Goldberg., *Genetic Algorithms in Search, Optimization, Machine Learning*. Boston, MA, USA: Addison-Wesley Longman Publishing Co., Inc, 2009.
[22] D. H. Luenberger, *Linear and Nonlinear Programming*. Englewood Cliffs, NJ, USA: Prentice-Hall, 1984.
[23] J. Proakis, *Digital Communications*., 4th ed. New York, NY, USA: McGraw-Hill, 2000.
[24] P. van Laarhoven and E. Aarts, *Simulated Annealing: Theory and Applications*. Norwell, MA, USA: Kluwer, 1987.

Amit Kumar Dutta (SM'XX) received the B.E. degree in electronics and tele-communication engineering from Bengal Engineering and Science University, India, in 2000. He is currently pursuing the Ph.D degree at the Department of ECE, Indian Institute of Science, India. AQ1

He worked in Texas Instrument (TI) Pvt. Ltd., India, from 2000 to 2009. During his career at TI, he worked on various design and test aspects of communication and entertainment related System-on-Chip. The works included digital VLSI design and its test, validation and characterization.

He is interested in the applications of statistical signal processing algorithms to wireless communication systems. His current research interests are on the various parameter estimation and signal detection for MIMO wireless receiver based on the Minimum Bit-Error-Ratio criterion.

K. V. S. Hari (M'92–SM'97) received the B.E. degree from Osmania University in 1983, M.Tech. degree from IIT Delhi in 1985, and the Ph.D. degree University of California at San Diego in 1990. Since 1992, he has been a Faculty Member at the Department of ECE, Indian Institute of Science (IISc), Bangalore, where he is currently a Professor and coordinates the activities of the Statistical Signal Processing Lab in the department. Currently, he is also an Affiliated Professor in the School of Electrical Engineering, KTH-Royal Institute of Technology, Stockholm, Sweden.

He has been a visiting faculty member at Stanford University, KTH-Royal Institute of Technology and Helsinki University of Technology (now Aalto Univ). He also worked at DLRL, Hyderabad, and at the R&D unit for Navigational Electronics, Osmania University.

His research interests are in developing signal processing algorithms for MIMO wireless communication systems, sparse signal recovery problems, indoor positioning and DOA estimation.

During his work at Stanford University, he worked on MIMO wireless channel modeling and is the coauthor of the WiMAX standard on wireless channel models for fixed-broadband wireless communication systems which proposed the Stanford University Interim (SUI) channel models. He is currently an Editor of the EURASIP's Journal on Signal Processing published by Elsevier and the Senior Associate Editor, Editorial Board of Sadhana (Indian Academy of Science Proceedings in Engineering Sciences). He is also an academic entrepreneur and is a cofounder of the company ESQUBE Communication Solutions, Bangalore.

Lajos Hanzo (F'08) received the bachelor's degree in electronics in 1976 and the doctoral degree in 1983. In 2009 he was awarded the honorary doctorate "Doctor Honoris Causa" by the Technical University of Budapest. During his 37-year career in telecommunications he has held various research and academic posts in Hungary, Germany and the UK. Since 1986 he has been with the School of Electronics and Computer Science, University of Southampton, U.K., where he holds the chair in telecommunications. He has successfully supervised more than 80 Ph.D. students, co-authored 20 John Wiley/IEEE Press books on mobile radio communications totalling in excess of 10 000 pages, published 1400+ research entries at IEEE Xplore, acted both as TPC and General Chair of IEEE conferences, presented keynote lectures and has been awarded a number of distinctions. Currently he is directing a 100-strong academic research team, working on a range of research projects in the field of wireless multimedia communications sponsored by industry, the Engineering and Physical Sciences Research Council (EPSRC) UK, the European Research Council's Advanced Fellow Grant and the Royal Society's Wolfson Research Merit Award. He is an enthusiastic supporter of industrial and academic liaison and he offers a range of industrial courses. He is also a Governor of the IEEE VTS. During 2008–2012 he was the Editor-in-Chief of the IEEE Press and a Chaired Professor also at Tsinghua University, Beijing. His research is funded by the European Research Council's Senior Research Fellow Grant. For further information on research in progress and associated publications please refer to http://www-mobile.ecs.soton.ac.uk.Dr.Hanzohasmorethan20 000+citations.

AUTHOR QUERIES

AUTHOR PLEASE ANSWER ALL QUERIES

AQ1 = Please provide membership history of author Amit Kumar Dutta.

END OF ALL QUERIES

Linear Transceiver Design for an Amplify-and-Forward Relay Based on the MBER Criterion

Amit Kumar Dutta, *Student Member, IEEE*, K. V. S. Hari, *Senior Member, IEEE*, and Lajos Hanzo, *Fellow, IEEE*

***Abstract*—A design methodology based on the Minimum Bit Error Ratio (MBER) framework is proposed for a non-regenerative Multiple-Input Multiple-Output (MIMO) relay-aided system to determine various linear parameters. We consider both the Relay-Destination (RD) as well as the Source-Relay-Destination (SRD) link design based on this MBER framework, including the precoder, the Amplify-and-Forward (AF) matrix and the equalizer matrix of our system. It has been shown in the previous literature that MBER based communication systems are capable of reducing the Bit-Error-Ratio (BER) compared to their Linear Minimum Mean Square Error (LMMSE) based counterparts. We design a novel relay-aided system using various signal constellations, ranging from QPSK to the general M-QAM and M-PSK constellations. Finally, we propose its sub-optimal versions for reducing the computational complexity imposed. Our simulation results demonstrate that the proposed scheme indeed achieves a significant BER reduction over the existing LMMSE scheme.**

***Index Terms*—Minimum bit error ratio (MBER), linear minimum mean square error (LMMSE), Relay, multiple-input multiple-output (MIMO), singular-value-decomposition (SVD).**

I. Introduction

RELAY-BASED communication systems have enjoyed considerable research attention due to their ability to provide a substantial spatial diversity gain with the aid of distributed nodes, hence potentially extending the coverage area and/or for reducing the transmit power [1], [2]. A pair of key protocols has been conceived for relay-aided systems, namely the regenerative [3], [4] and the non-regenerative [5], [6] protocols. In the regenerative scenario, the relay node (RN) decodes the signal and then forwards it after amplification to the destination node (DN) (also known as a decode-forward relay), while maintaining the same total relay- plus source-power as the original non-relaying scheme. By contrast, in the case of non-regenerative relaying, the RN only amplifies the signal received from the source node (SN) and then forwards it to the DN without any decoding (also known as an amplify-and-forward relay), again, without increasing the power of the original direct SN-DN pair. Non-regenerative relaying is invoked for applications, where both low latency and low complexity are required.

Multiple-input multiple-output (MIMO) techniques may be beneficially combined with relaying for further increasing both the attainable spectral efficiency and the signal reliability. The non-regenerative relay involves the design of both the Amplify-and-Forward (AF) matrix at the RN and the linear equalizer design at the DN, or any precoder matrix at the SN, subject to the above total SN and (or) RN power constraints. Various Cost Functions (CF) have been proposed for optimizing these matrices, such as the Linear Minimum Mean Square Error (LMMSE) [7]–[10] and the Maximum Capacity (MC) [11], [12] CFs, etc. However, the direct minimization of the Bit-Error-Ratio (BER) at the DN has not as yet been fully explored in the context of designing the various parameters of non-regenerative MIMO-aided relaying, although a BER based RN design was proposed In reply to: [13] for a single-antenna scenario. Hence, the work in [13] does not deal with the design of precoder, AF and linear equalizers as matrices due to the consideration of single antenna at SN, RN and DN. Though, a Minimum Bit Error Ratio (MBER) CF based MIMO-aided relay design [14] was provided for a cooperative, non-regenerative relay employing distributed space time coding, it was based on the classic BPSK signal sets. This work assumes the power allocation matrix to be diagonal and no RN power constraint was used in the optimization problem. In this case of [14], the relay power was normalized after determining the diagonal AF and precoder matrices with unconstrained optimization problem, which leads to a sub-optimal solution.

The benefit of MBER-based linear system design has been well studied in literature. To elaborate a little further, the MBER CF directly minimizes the BER [15]. Previous literature has shown that a sophisticated system design based on this criterion is capable of outperforming its LMMSE counterpart in terms of the attainable BER. Owing to its benefits, it has been used for the design of a linear equalizer [15], for the precoder matrix [16] and for various other MIMO, SDMA as well as OFDM systems conceived for achieving the best BER performance [17]–[19] at the of higher computational complexity. MBER based linear receiver design has also been shown to be very effective in terms of BER performance in the rank-deficient case, where conventional LMMSE-based receiver fails to perform significantly [20].

Manuscript received January 30, 2014; revised June 26, 2014; accepted August 12, 2014. The associate editor coordinating the review of this paper and approving it for publication was M. Uysal.

A. K. Dutta and K. V. S. Hari are with the Department of Electrical Communication Engineering, Indian Institute of Science, Bangalore 560012, India (e-mail: amitkdatta@ece.iisc.ernet.in; hari@ece.iisc.ernet.in).

L. Hanzo is with the Department of Electronics and Computer Science, University of Southampton, Southampton SO17 1BJ, U.K. (e-mail: lh@ecs.soton.ac.uk).

Digital Object Identifier 10.1109/TCOMM.2014.2350973

Scope and contribution: Against this background based on the MBER CF, we design of a new non-regenerative MIMO-aided relaying system, which comprises a SN, a RN and a DN. We assume a half duplex system at the RN, where one time slot is used for receiving from the SN and another for forwarding it to the DN. No SN-RN transmission takes place during the RN-DN transmission. In this work, we consider the joint design of the SN's transmit precoder, the RN's AF matrix and the DN's linear equalizer matrix based on the MBER CF subject to the above total RN-SN power constraints. The performance of the proposed scheme is evaluated and compared to that of the existing LMMSE based method. The main contributions of this treatise are as follows:

1) A CF is conceived for the design of the RN-DN and the SN-RN-DN links of a non-regenerative relaying system based on the MBER CF subject to the SN and (or) RN power constraints. The MBER CF is formulated for various data constellations, ranging from BPSK to the general M-QAM and M-PSK constellations. Naturally, the specific choice of the constellation fundamentally influences the MBER CF [15], [17]–[19]. We jointly determine the precoder, AF and equalizer matrices based on this MBER CF under a source and relay power constraint. The existing MIMO MBER solutions are designed for unconstrained scenarios and hence this constrained MBER optimization poses specific challenges. Therefore, we have conceived both the heuristic constrained binary Genetic Algorithm (GA) [21] and the Projected Steepest Descent (PSD) [22] algorithm for determining these parameters.
2) A suboptimal method is also proposed for reducing the number of variables using the Singular-Value-Decomposition (SVD) approach, which allows the optimization problem to be decomposed into multiple parallel optimization problems. The key contribution here is that we propose to split the complete constrained optimization problem into unconstrained parallel optimization problems except for one of the cases.
3) The Cost Function (CF) of M-PSK constellation has been approximated for the sake of conceiving a more tractable form for the MIMO-aided relaying system considered. This approximation can also be used for classic MIMO scenarios.
4) An impediment of the MBER CF is however its high computational complexity compared to its LMMSE counterpart [15]. To mitigate this, we have conceived a low-complexity data detection scheme for the MBER method with the aid of the phase rotation of the constellation in the context of rotationally invariant QPSK and M-PSK constellations. This scheme can be equally applicable to any other MIMO system design based on the MBER criterion.
5) An approximate complexity analysis is performed for the MBER scheme under various constrained optimization methods such as the GA and PSD. This step-by-step analysis may be readily applied to other MBER solutions.

Notation: Bold upper and lower case letters denote matrices and vectors, respectively. The superscripts $(\cdot)^T$ and $(\cdot)^H$ denote the transpose and the conjugate transpose of a matrix, respectively. $\mathbb{E}[\cdot]$ denotes the expectation, while $\mathbf{I}_N$ denotes a $(N \times N)$-element identity matrix. $Tr[\cdot]$ represents the trace of a matrix. A diagonal matrix is denoted by $diag\{a_1, a_2, \ldots, a_N\}$, where a_n denotes the nth diagonal element. $vec(\mathbf{A})$ is the vectorization of the matrix $\mathbf{A}$ with columns stacked one-by-one.

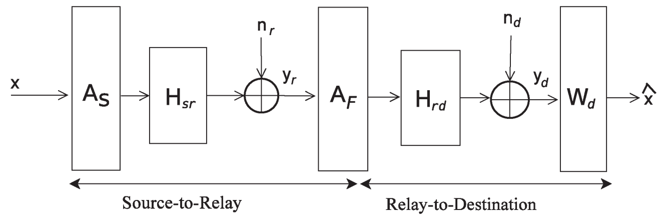

Fig. 1. Single relay system with multiple input-output antennas at source, relay, and destination.

II. System Model

We consider a communication system consisting of a SN, a RN and a DN having N_s, N_r, and N_d antennas, respectively, as shown in Fig. 1. It is assumed that there is no Line-Of-Sight (LOS) component between the SN and the DN. Both the SN-RN and the RN-DN channel matrices are assumed to be those of flat-fading channels, which are denoted as $\mathbf{H}_{sr} \in \mathbb{C}^{N_r \times N_s}$ and $\mathbf{H}_{rd} \in \mathbb{C}^{N_d \times N_r}$, respectively. The symbol vector transmitted from the SN before precoding is denoted as $\mathbf{x} \in \mathbb{C}^{N_x \times 1}$ with N_x being the length of the input vector. We assume $\mathbf{A}_S \in \mathbb{C}^{N_S \times N_x}$ to be the precoding matrix at the SN. The average transmitted power is constrained to $P_t = \mathbb{E}[\mathbf{s}^H\mathbf{s}]$ with $\mathbf{s} \triangleq \mathbf{A}_S\mathbf{x}$, which is assumed to be the same for all symbols at the SN. Hence, we have the transmit power constraint as $P_t \triangleq \mathbb{E}\|\mathbf{A}_S\mathbf{x}\|^2 = \sigma_x^2 Tr(\mathbf{A}_S\mathbf{A}_S^H)$ and the transmit data covariance matrix is $\mathbf{R}_S \triangleq \mathbb{E}(\mathbf{s}\mathbf{s}^H) = (P_t/N_x)(\mathbf{A}_S\mathbf{A}_S^H)$, where $\sigma_x^2 = (P_t/N_x)$ is the signal power of each data x_i. The noise vectors at the RN and the DN are $\mathbf{n}_r \in \mathbb{C}^{N_r \times 1}$ and $\mathbf{n}_d \in \mathbb{C}^{N_d \times 1}$, respectively, which are assumed to be zero mean, circularly symmetric complex i.i.d Gaussian vectors having the covariance matrices of $\sigma_r^2\mathbf{I}_{N_r}$ and $\sigma_d^2\mathbf{I}_{N_d}$, respectively. We consider a classic half duplex system. Hence, in the first time slot, the SN transmits a source vector $\mathbf{s}$ and the vector $\mathbf{y}_r \in \mathbb{C}^{N_r \times 1}$, received at the RN is given by,

$$\mathbf{y}_r = \mathbf{H}_{sr}\mathbf{s} + \mathbf{n}_r. \tag{1}$$

During the next time slot, the relay would multiply the received vector $\mathbf{y}_r$ with the AF matrix $\mathbf{A}_F \in \mathbb{C}^{N_r \times N_r}$ and then forwards it to the DN. Let us assume that $\mathbf{y}_F \triangleq \mathbf{A}_F\mathbf{y}_r = \mathbf{A}_F(\mathbf{H}_{sr}\mathbf{s} + \mathbf{n}_r)$. We impose the RN transmit power restriction of $\mathbb{E}[\mathbf{y}_F^H\mathbf{y}_F] \leq P_r$, where P_r is the RN's transmit power. Assuming that the SN's transmitted signal and the noise are independent, the RN's power can be calculated as,

$$\begin{aligned}\mathbb{E}\left[\mathbf{y}_f^H\mathbf{y}_f\right] &= Tr\left\{\mathbb{E}\left(\mathbf{A_F}(\mathbf{H}_{sr}\mathbf{s}+\mathbf{n}_r)(\mathbf{H}_{sr}\mathbf{s}+\mathbf{n}_r)^H\mathbf{A}_F^H\right)\right\}\\ &= Tr\left\{\mathbf{A}_F\left(\sigma_x^2\mathbf{H}_{sr}\mathbf{A}_S\mathbf{A}_S^H\mathbf{H}_{sr}^H + \sigma_r^2\mathbf{I}_{N_r}\right)\mathbf{A}_F^H\right\}\\ &\leq P_r, \end{aligned} \tag{2}$$

TABLE I
REQUIREMENT OF CSI AT VARIOUS NODES FOR MBER CRITERION BASED RELAY DESIGN

Relay design type	*SN*	*RN*	*DN*
RN-DN		$\mathbf{H}_{sr}$, $\mathbf{H}_{rd}$	$\mathbf{H}_{rd}$
SN-RN-DN (Sub-optimal)	$\mathbf{H}_{sr}$	$\mathbf{H}_{sr}$, $\mathbf{H}_{rd}$	$\mathbf{H}_{rd}$
SN-RN-DN (Optimal)		$\mathbf{H}_{sr}$, $\mathbf{H}_{rd}$	$\mathbf{H}_{rd}$

where $\mathbb{E}\{\mathbf{x}\mathbf{x}^H\} = \sigma_x^2 \mathbf{I}_{N_x}$. Now, the signal received at the DN, $\mathbf{y}_d \in \mathbb{C}^{N_d \times 1}$ is obtained as,

$$\begin{aligned}\mathbf{y}_d &= \mathbf{H}_{rd}\mathbf{y}_f + \mathbf{n}_d \\ &= \mathbf{H}_{rd}\mathbf{A}_F\left(\mathbf{H}_{sr}\mathbf{s} + \mathbf{n}_r\right) + \mathbf{n}_d \\ &= \{\mathbf{H}_{rd}\mathbf{A}_F\mathbf{H}_{sr}\mathbf{A}_S\}\,\mathbf{x} + \{\mathbf{H}_{rd}\mathbf{A}_F\mathbf{n}_r + \mathbf{n}_d\} \\ &\triangleq \mathbf{H}\mathbf{x} + \mathbf{n},\end{aligned} \tag{3}$$

where $\mathbf{H} \triangleq \mathbf{H}_{rd}\mathbf{A}_F\mathbf{H}_{sr}\mathbf{A}_S$ and $\mathbf{n} \triangleq \mathbf{H}_{rd}\mathbf{A}_F\mathbf{n}_r + \mathbf{n}_d$. The new effective noise vector $\mathbf{n}$ is a colored zero-mean Gaussian vector with the distribution of $CN(\mathbf{0}, \mathbf{C}_n)$, where $\mathbf{C}_n \in \mathbb{C}^{N_d \times N_d}$ is the new noise covariance matrix, which may be expressed as,

$$\begin{aligned}\mathbf{C}_n &= \mathbb{E}[\mathbf{n}\mathbf{n}^H] \\ &= \sigma_d^2\mathbf{I}_{N_d} + \sigma_r^2\mathbf{H}_{rd}\mathbf{A}_F\mathbf{A}_F^H\mathbf{H}_{rd}^H.\end{aligned} \tag{4}$$

At the DN, we employ a linear equalizer for detecting the transmitted symbol $\mathbf{x}$. We assume that the equalizer matrix at the DN is $\mathbf{W}_d \in \mathbb{C}^{N_x \times N_d}$, hence the estimated value of $\mathbf{x}$ is $\hat{\mathbf{x}} = \mathbf{W}_d^H\mathbf{y}_d$.

Note: The RN determines the $\mathbf{A}_S$, $\mathbf{A}_F$ and $\mathbf{W}_d$ matrices jointly. Thus, we assume that the RN has the complete knowledge of $\mathbf{H}_{sr}$ and $\mathbf{H}_{rd}$, while the DN knows only $\mathbf{H}_{rd}$ and feeds it back to the RN through a reliable communication channel. The SN has to know the matrix $\mathbf{H}_{sr}$ only for the case of the sub-optimal SN-RN-DN (SRD) relay design to be described later. We refer "sub-optimal", when Singular-Value-Decomposition (SVD) based structure is assumed for AF and source precoder matrices. In this case, only the singular values of these matrices need to be determined. By contrast, "optimal" refers to the case, where full complex AF and source precoder matrices need to be determined. Thus, for "optimal" case, SN need not to know the $\mathbf{H}_{sr}$ as the whole solution of the precoder will be sent back to SN by RN. For the sub-optimal case, the SN needs to reconstruct the precoder matrix from the SVD component of the $\mathbf{H}_{sr}$ matrix. Table I shows the parameter knowledge requirements at different nodes, which are consistent with [9], except for our proposed optimal SN-RN-DN link design. We first develop the RN-DN link and then extend it to the SN-RN-DN link. For the RN-DN system, only the matrices $\mathbf{A}_F$ and $\mathbf{W}_d$ have to be determined subject to the above RN power constraints. By contrast, for the SN-RN-DN system, the matrices $\mathbf{A}_S$, $\mathbf{A}_F$ and $\mathbf{W}_d$ are determined subject to both the SN and the RN power constraints.

III. MBER BASED RELAY-DESTINATION DESIGN

We first consider the RN-DN link design, which involves the design of both the AF matrix $\mathbf{A}_F$ and of the equalizer matrix $\mathbf{W}_d$. Various existing CFs, such as the LMMSE [7], the Maximum Capacity (MC) [11] have been considered to design both $\mathbf{A}_F$ and $\mathbf{W}_d$. In this treatise, we propose a solution based on the MBER CF for jointly determining these matrices. For the RN-DN link, the precoder matrix $\mathbf{A}_S$ is fixed to $\mathbf{I}_{N_s}$ along with $N_s = N_x$. The total transmitted power is fixed to $P_t = \sigma_x^2 N_s$. The signals received at the RN and the DN are $\mathbf{y}_r = \mathbf{H}_{sr}\mathbf{x} + \mathbf{n}_r$ and $\mathbf{y}_d = \mathbf{H}_{rd}\mathbf{A}_F\mathbf{H}_{sr}\mathbf{x} + \mathbf{H}_{rd}\mathbf{A}_F\mathbf{n}_r + \mathbf{n}_d$, respectively. The RN's power becomes $Tr\{\mathbf{A}_F(\sigma_x^2\mathbf{H}_{sr}\mathbf{H}_{sr}^H + \sigma_r^2\mathbf{I}_{N_r})\mathbf{A}_F^H\}$. In the current context, the MBER CF directly minimizes the BER of the system at the DN. We first consider the CF based on the BPSK constellation and then we extend it to the M-QAM and M-PSK constellations.

Note: We will be formulating the cost function (CF) as the symbol error ratio (SER). With a slight inaccuracy of terminology, we refer to the MBER as that of minimizing the SER in the subsequent sections. It is to be noted that minimizing SER will also lead to minimization of BER as $BER \approx SER/\log_2(M)$ for most of the constellations [23].

A. Cost Function

Let us assume that $P_{e,i}$ denotes the SER, when detecting x_i (the ith component of $\mathbf{x}$) at the DN. If every x_i is detected independently, the average probability of a symbol error associated with detecting the complete vector $\mathbf{x}$ is given by,

$$P_e = \frac{1}{N_s}\sum_{i=1}^{N_s} P_{e,i}. \tag{5}$$

We constrain the RN's transmission power to P_r and formulate $P_{e,i}$ associated with various constellations. Furthermore, we would simplify the expression of $P_{e,i}$ using various sub-optimal approaches. The optimization problem is stated as follows:

$$\begin{aligned}\mathbf{A}_F^{mber}, \mathbf{W}_d^{mber} &= \underset{\mathbf{A}_F,\mathbf{W}_d}{arg}\ \min\ P_e(\mathbf{A}_F, \mathbf{W}_d) \\ s.t\ Tr&\left\{\mathbf{A}_F\left(\sigma_x^2\mathbf{H}_{sr}\mathbf{H}_{sr}^H + \sigma_r^2\mathbf{I}_{N_r}\right)\mathbf{A}_F^H\right\} \le P_r.\end{aligned} \tag{6}$$

Note: Equation (6) describes a constrained optimization problem, where the constraint is with respect to the RN's transmitter power. Here, all $P_{e,i}$ for $i = 1, 2 \ldots, N_s$ are optimized together to arrive at the optimized $\mathbf{A}_F$ and $\mathbf{W}_d$ matrices. Explicitly, Equation (6) is simultaneously optimized over $(N_r^2 + N_s \times N_d)$ number of complex-valued variables. This is because the $\mathbf{A}_F$ matrix has N_r^2 number of complex entries, while the $\mathbf{W}_d$ matrix has $(N_s \times N_d)$ complex entries. Therefore, the related optimization problem has a high computational complexity. Hence, we now propose a suboptimal technique for reducing the number of variables to be optimized.

1) Sub-Optimal Approaches for Reducing Both the Number of Variables and the Complexity: Let us first decompose $\mathbf{H}_{sr}$ and $\mathbf{H}_{rd}$ using the Singular Value Decomposition (SVD) as $\mathbf{H}_{sr} = \mathbf{U}_1\mathbf{\Sigma}_{sr}\mathbf{V}_1^H$ and $\mathbf{H}_{rd} = \mathbf{U}_2\mathbf{\Sigma}_{rd}\mathbf{V}_2^H$ respectively, where $\mathbf{U}_1 \in \mathbb{C}^{N_r \times N_r}$, $\mathbf{V}_1 \in \mathbb{C}^{N_s \times N_s}$, $\mathbf{U}_2 \in \mathbb{C}^{N_d \times N_d}$, $\mathbf{V}_2 \in \mathbb{C}^{N_r \times N_r}$ are unitary matrices, whereas $\mathbf{\Sigma}_{sr} \in \mathbb{R}^{N_r \times N_S}$ and $\mathbf{\Sigma}_{rd} \in \mathbb{R}^{N_d \times N_r}$ are matrices having singular values of $\sigma_{sr,i}$ for $i = 1, 2, \ldots, \min(N_r, N_s)$ and $\sigma_{rd,i}$ for $i = 1, 2, \ldots, \min(N_d, N_r)$ in a descending order on the main diagonal, respectively. We also assume that $\mathbf{w}_i$ is the ith column of $\mathbf{W}_d$ for $i = 0, 1, \ldots, N_d - 1$.

We now propose a pair of computational complexity reduction techniques.

1) We use the SVD of the matrix $\mathbf{A}_F$, which has been shown to be optimal in the Mean Square Error (MSE) sense [7]. However, this decomposition may not be optimal in the MBER sense. The assumed structure of $\mathbf{A}_F$ is defined as,

$$\mathbf{A}_F \triangleq \mathbf{V}_2 \mathbf{\Sigma}_F \mathbf{U}_1^H \tag{7}$$

where the unitary matrices $\mathbf{V}_2$ and $\mathbf{U}_1$ have been defined earlier. Furthermore, $\mathbf{\Sigma}_F \in \mathbb{R}^{N_r \times 1}$ is the singular value matrix of $\mathbf{A}_F$, which has the singular values of $\sigma_{f,i}$ for $i = 1, 2, \ldots, N_r$. This reduces the N_r^2 number of complex variables to just N_r real variables.

2) We propose to optimize each $P_{e,i}$ in parallel. This reduces the optimization complexity for each index i. We propose furthermore that for the k^{th} index $i = k$, $P_{e,k}$ is optimized with respect to both $\mathbf{\Sigma}_F$ and $\mathbf{w}_k$. The obtained $\mathbf{\Sigma}_F$ is then used for the rest of the $P_{e,i}$ values for $i = 1, 2, 3, \ldots, k-1, k+1, \ldots, N_s$ as a given parameter. It is noted that the RN's power constraint is not a function of any of the equalizers for $i = 1, 2, 3, \ldots, k-1, k+1, \ldots, N_s$, hence the RN's power constraint is not considered thereafter. As a benefit, a valuable computational complexity reduction is achieved, since we only have to deal with $(N_r + N_d)$ number of complex variables for $i = k$ and then only with N_d complex variables for rest of i values without any RN power constraint. Furthermore, for $i = 1, 2, 3, \ldots, k-1, k+1, \ldots, N_s$ onward, the computation of $\mathbf{w}_i$ can be performed in parallel, which facilitates the design of a larger chip capable of operating at a higher bit-rate, regardless of the specific choice of optimization method.

By exploiting the SVD structure based assumption concerning $\mathbf{A}_F$, $\mathbf{H}$ can be reduced to

$$\begin{aligned}
\mathbf{H} &= \mathbf{H}_{rd} \mathbf{A}_F \mathbf{H}_{sr} \\
&= \mathbf{U}_2 \mathbf{\Sigma}_{rd} \mathbf{V2}^H \mathbf{V}_2 \mathbf{\Sigma}_F \mathbf{U1}^H \mathbf{U}_1 \mathbf{\Sigma}_{sr} \mathbf{V1}^H \\
&= \mathbf{U}_2 \mathbf{\Sigma}_{rd} \mathbf{\Sigma}_F \mathbf{\Sigma}_{sr} \mathbf{V1}^H \\
&\triangleq \mathbf{U}_2 \mathbf{\Sigma} \mathbf{V}_1^H,
\end{aligned} \tag{8}$$

where $\mathbf{\Sigma} \triangleq \mathbf{\Sigma}_{rd} \mathbf{\Sigma}_F \mathbf{\Sigma}_{sr}$. Let us now compute the RN's power under the assumed structure of $\mathbf{A}_F$ as follows

$$\begin{aligned}
\mathbb{E}\left[\mathbf{y}_f^H \mathbf{y}_f\right] &= Tr\left\{\mathbf{A}_F \left(\sigma_x^2 \mathbf{H}_{sr} \mathbf{H}_{sr}^H + \sigma_r^2 \mathbf{I}_{N_r}\right) \mathbf{A}_F^H\right\} \\
&= Tr\left\{\mathbf{V}_2 \mathbf{\Sigma}_F \left(\sigma_x^2 \mathbf{\Sigma}_{sr} \mathbf{\Sigma}_{sr}^H + \sigma_r^2 \mathbf{I}_{N_r}\right) \mathbf{\Sigma}_F^H \mathbf{V}_2^H\right\} \\
&= Tr\left\{\mathbf{\Sigma}_F \left(\sigma_x^2 \mathbf{\Sigma}_{sr} \mathbf{\Sigma}_{sr}^H + \sigma_r^2 \mathbf{I}_{N_r}\right) \mathbf{\Sigma}_F^H\right\} \\
&= \sum_{i=1}^{N_r} \sigma_{f,i}^2 \left(\sigma_x^2 \sigma_{sr,i}^2 + \sigma_r^2\right) \le P_r.
\end{aligned} \tag{9}$$

Explicitly, the RN's power constraint becomes less complex, since it does not involve any complex-valued matrix operations. In a similar way, we now re-calculate the covariance matrix $\mathbf{C}_n$ of the composite noise, as perceived at the DN. Let us assume that $\mathbf{A} \triangleq \mathbf{H}_{rd} \mathbf{A}_F \mathbf{A}_F^H \mathbf{H}_{rd}$. Thus, we calculate $\mathbf{A}$ as follows

$$\begin{aligned}
\mathbf{A} &= \mathbf{H}_{rd} \mathbf{A}_F \mathbf{A}_F^H \mathbf{H}_{rd} \\
&= \mathbf{U}_2 \mathbf{\Sigma}_{rd} \mathbf{V}_2^H \mathbf{V}_2 \mathbf{\Sigma}_F \mathbf{\Sigma}_F^H \mathbf{V}_2^H \mathbf{V}_2 \mathbf{\Sigma}_{rd}^H \mathbf{U}_2^H \\
&= \mathbf{U}_2 \mathbf{\Sigma}_{rd} \mathbf{\Sigma}_F \mathbf{\Sigma}_F^H \mathbf{\Sigma}_{rd}^H \mathbf{U}_2^H \\
&\triangleq \mathbf{U}_2 \mathbf{\Sigma}_A \mathbf{U}_2^H,
\end{aligned} \tag{10}$$

where $\mathbf{\Sigma}_A \triangleq \mathbf{\Sigma}_{rd} \mathbf{\Sigma}_F \mathbf{\Sigma}_F^H \mathbf{\Sigma}_{rd}^H$. Upon substituting Equation (10) into Equation (4), we arrive at $\mathbf{C}_n = \sigma_d^2 \mathbf{I}_{N_d} + \sigma_r^2 \mathbf{U}_2 \mathbf{\Sigma}_A \mathbf{U}_2^H$. Our new optimization problem is then redefined as follows

$$\begin{aligned}
&\text{For i = k :} \\
&\mathbf{\Sigma}_F^{mber}, \mathbf{w}_k^{mber} = \underset{\mathbf{\Sigma}_F, \mathbf{w}_k}{arg \min}\ P_{e,k}(\mathbf{\Sigma}_F, \mathbf{w}_k) \\
&\qquad s.t \sum_{i=1}^{N_r} \sigma_{f,i}^2 \left(\sigma_x^2 \sigma_{sr,i}^2 + \sigma_r^2\right) \le P_r.
\end{aligned} \tag{11}$$

$$\begin{aligned}
&\text{For i} = 1, 2, 3, \ldots, \text{k} - 1, \text{k} + 1, \ldots, \text{N_s :} \\
&\mathbf{w}_i^{mber} = \underset{\mathbf{w}_i}{arg \min}\ P_{e,i}(\mathbf{\Sigma}_F^{mber}, \mathbf{w}_i).
\end{aligned} \tag{12}$$

2) MBER CF Associated With the BPSK Constellation: We first formulate the MBER CF for the BPSK constellation for the sake of conceptual simplicity and then extend it to the M-QAM and M-PSK constellations. Let us assume that $\mathbf{w}_i$ is the ith column of the DN's equalizer matrix $\mathbf{W}_d$. If $\hat{x}_i$ is the estimate of x_i for the BPSK constellation, we arrive at the expression of $P_{e,i}^{BPSK}$ as follows [15]:

$$\begin{aligned}
P_{e,i}^{BPSK} &= P_r\left\{x_i \Re\{\hat{x}_i\} < 0\right\} \\
&= P_r\left\{\Re\{x_i (\mathbf{w}_i)^H \mathbf{H}\mathbf{x} + x_i (\mathbf{w}_i)^H \mathbf{n}\} < 0\right\} \\
&= \mathbb{E}_{\mathbf{x}}\left[P_r\left\{\Re\{x_i (\mathbf{w}_i)^H \mathbf{H}\mathbf{x} + x_i (\mathbf{w}_i)^H \mathbf{n}\} < 0\right\} |\mathbf{x}\right] \\
&= \mathbb{E}_{\mathbf{x}}\left[Q\left(\frac{\Re\left[(\mathbf{w}_i)^H \mathbf{H}\mathbf{x} x_i\right]}{\sqrt{\frac{1}{2}(\mathbf{w}_i)^H \mathbf{C}_n \mathbf{w}_i}}\right)\right] \\
&= \frac{1}{L}\sum_{j=1}^{L} Q\left(\frac{\Re\left[(\mathbf{w}_i)^H \mathbf{H}\mathbf{x}_j x_i\right]}{\sqrt{\frac{1}{2}(\mathbf{w}_i)^H \mathbf{C}_n \mathbf{w}_i}}\right),
\end{aligned} \tag{13}$$

where $L = 2^{N_s}$ represents the total number of unique realizations of $\mathbf{x}$, while $\mathbf{x}_j$ is the jth such realization of $\mathbf{x}$.

3) The MBER CF Associated With the M-QAM Constellation: For the M-QAM constellation, we assume that the distance between any two adjacent constellation points along either the real or the imaginary axis is $2a$ for $a > 0$.

The M-QAM constellation can thus be interpreted as a pair of PAM sequences of length $\sqrt{M}$ along the real and imaginary axes. Thus, the SER of the M-QAM constellation is derived as,

$$P_{e,i}^{QAM} = 1 - P_{c,i}^{R} \cdot P_{c,i}^{I} \tag{14}$$

where $P_{c,i}^{R}$, $P_{c,i}^{I}$ are the probability of correct decision for the QAM signal along the real and imaginary axes, respectively. For computational simplicity, we assume that the decision region of each point along either the real or imaginary axis is bounded by the length $2a$, though the terminal points have larger range for decision region. This way, we only make each decision region uniform and restrictive to an extent. Let us now define $L_1 = M^{((N_s-1)/2)}$. Now, $P_{c,i}^{R}$, $P_{c,i}^{I}$ are derived in Equations (15) and (16), respectively (see equation at bottom of page).

4) The MBER CF Associated With the M-PSK Constellation: For the M-PSK signal constellation set, each point is assumed to be on a unit circle and represented as $e^{j(2\pi m/M)}$ for $m = 0, 1, \ldots, M-1$. Note that the real and imaginary components of the DN's equalizer output noise, $\mathbf{w}_i^H \mathbf{n}$, are correlated Gaussian random variables. For computational simplicity, we invoke an approximation and we whiten the noise by assuming $\mathbf{A}_F$ to have the proposed SVD form of Equation (7). We commence by using $\mathbf{C}_n$ from Equation (4) as,

$$\mathbf{C}_n = \mathbf{\Sigma}_{rd} \mathbf{\Sigma}_F \mathbf{\Sigma}_F^T \mathbf{\Sigma}_{rd}^T + \sigma_d^2 \mathbf{I}_{N_d}. \tag{17}$$

Thus, the ith diagonal element of $\mathbf{C}_n$ is $[\mathbf{C}_n]_{ii} = \sigma_d^2 + \sigma_{rd,i}^2 \sigma_{f,i}^2$. The noise whitening matrix is defined as $\mathbf{C}_s \triangleq \mathbf{C}_n^{-(1/2)}$ with $[\mathbf{C}_s]_{ii} = (1/\sqrt{\sigma_d^2 + \sigma_{rd,i}^2 \sigma_{f,i}^2})$. Therefore, the modified output vector received at the DN is defined as,

$$\begin{aligned} \mathbf{y}_s &= \mathbf{C}_s \mathbf{y}_d \\ &= \mathbf{C}_s \mathbf{H} \mathbf{x} + \mathbf{n}_s \\ &= \mathbf{H}_s \mathbf{x} + \mathbf{n}_s, \end{aligned} \tag{18}$$

with $\mathbf{n}_s \in \mathbb{C}^{N_s \times 1}$ being the zero-mean i.i.d Gaussian random vector with each component having a unit variance. Let us assume that $\mu_i^R \triangleq \Re\{\mathbf{w}_i^H \mathbf{H}_s \mathbf{x}\}$ and $\mu_i^I \triangleq \Im\{\mathbf{w}_i^H \mathbf{H}_s \mathbf{x}\}$, where $\mathbf{w}_i$ is the ith equalizer as defined earlier. Let furthermore r_1 and r_2 be the real and imaginary components of the equalizer output. Their joint probability is calculated as [23],

$$p_{r_1,r_2,i} = \frac{1}{2\pi\sigma^2} e^{-\left\{(r_1-\mu^R)^2 + (r_2-\mu^I)^2\right\}/2\sigma^2} \tag{19}$$

where $\sigma^2 = (1/2)\mathbf{w}_i^H \mathbf{w}_i$. Let us now define $V \triangleq \sqrt{r_1^2 + r_2^2}$ and the angle $\theta \triangleq \tan^{-1}((r_2/r_1))$. Thus, the probability of θ for the ith symbol is obtained as [23]

$$p_{\theta,i} = \frac{1}{2\pi\sigma^2} e^{-\left(\mu_i^R \sin(\theta) - \mu_i^I \cos(\theta)\right)^2/2\sigma^2} \times \int_0^\infty V e^{-\left(V - \mu_i^I sin(\theta) - \mu_i^R cos(\theta)\right)^2/2\sigma^2} dV. \tag{20}$$

At the higher SNR values, an approximation has been proposed for Equation (20) in [23] as follows,

$$p_{\theta,i} \approx \frac{1}{\sqrt{2\pi\sigma^2}} \left(\mu_i^I sin(\theta) + \mu_i^R cos(\theta)\right) \times e^{-\left(\mu_i^R \sin(\theta) - \mu_i^I \cos(\theta)\right)^2/2\sigma^2}, \tag{21}$$

with $|\theta| \leq \pi/2$ and $|\theta| << 1$. Equation (21) is valid for $m = 0$. This suggests that any constellation point at the ith position of $\mathbf{x}$ can be rotated to the one corresponding to $m = 0$. Hence, we may conceive a scheme by exploiting the circular constellation of M-PSK, where the SER has to be found for the constellation point corresponding to $m = 0$. Thus, $\mathbf{w}_i$ is determined by minimizing the probability of this particular symbol error only. We then create M rotated versions of $\mathbf{y}_d$ as $\mathbf{y}_d^m = e^{-m\pi/M} \mathbf{I}_{N_d} \mathbf{y}_d$ for $m = 0, 1, \ldots, M-1$. The estimated constellation point $(\mathbf{w}_i^H \mathbf{y}_d^m)$ is then the one corresponding to any of the M number of $\mathbf{y}_d^m$ variables giving the minimum absolute angle.

$$P_{c,i}^{R} = \frac{1}{L_1} \sum_{j=1}^{L_1} \sum_{m=-(\sqrt{M}-1), m\ odd}^{\sqrt{M}-1} \left[Q\left(\frac{ma - a - \Re\left[(\mathbf{w}_i)^H \mathbf{H} \mathbf{x}_j\right]}{\sqrt{\frac{1}{2}(\mathbf{w}_i)^H \mathbf{C}_n \mathbf{w}_i}} \right) - Q\left(\frac{ma + a - \Re\left[(\mathbf{w}_i)^H \mathbf{H} \mathbf{x}_j\right]}{\sqrt{\frac{1}{2}(\mathbf{w}_i)^H \mathbf{C}_n \mathbf{w}_i}} \right) \right] \tag{15}$$

$$P_{c,i}^{I} = \frac{1}{L_1} \sum_{j=1}^{L_1} \sum_{m=-(\sqrt{M}-1), m\ odd}^{\sqrt{M}-1} \left[Q\left(\frac{ma - a - \Im\left[(\mathbf{w}_i)^H \mathbf{H} \mathbf{x}_j\right]}{\sqrt{\frac{1}{2}(\mathbf{w}_i)^H \mathbf{C}_n \mathbf{w}_i}} \right) - Q\left(\frac{ma + a - \Im\left[(\mathbf{w}_i)^H \mathbf{H} \mathbf{x}_j\right]}{\sqrt{\frac{1}{2}(\mathbf{w}_i)^H \mathbf{C}_n \mathbf{w}_i}} \right) \right] \tag{16}$$

Note: This technique imposes a low computational complexity for the following reasons.

1) Since, we consider the SER only for $m = 0$, the number of computational loops required for calculating the SER will be reduced to M^{N_s-1} from M^{N_s} per iteration.
2) Since, the SER of each constellation point requires a unique representation in terms of the Gaussian error function $Q(\cdot)$, the complexity of calculating all of them is high. However, for our low-complexity solution, we only have to calculate the SER for a single constellation point corresponding to $m = 0$.

The SER of the ith symbol of $\mathbf{x}$ is then formulated for our low-complexity method as

$$P_{e,i}^{PSK} = 1 - \frac{1}{L_2}\sum_{l=1}^{L_2}\int_{-\pi/M}^{\frac{\pi}{M}} p_{\theta,i}d\theta$$
$$= \frac{1}{L_2}\sum_{l=1}^{L_2} Q\left[\frac{\mu_{i,l}^R \sin\left(\frac{\pi}{M}\right) - \mu_{i,l}^I \cos\left(\frac{\pi}{M}\right)}{\sigma}\right]$$
$$+ \frac{1}{L_2}\sum_{l=1}^{L_2} Q\left[\frac{\mu_{i,l}^I \cos\left(\frac{\pi}{M}\right) + \mu_{i,l}^R \sin\left(\frac{\pi}{M}\right)}{\sigma}\right], \quad (22)$$

where $L_2 = M^{N_s-1}$ and $\mu_{i,l}^R$ or $\mu_{i,l}^I$ represent the values of μ_i^R or μ_i^I (as defined earlier) corresponding to the lth realization of $\mathbf{x}$, respectively.

IV. MBER Based Source-Relay-Destination Link Design

Let us now consider the design of the SRD link based on the MBER CF. This involves a transmit precoder (TPC) matrix design at the SN in addition to the AF matrix of the RN and the equalizer matrix of the DN. We also have to obey the power constraint at the SN involving the TPC matrix in addition to the RN power constraint. The TPC, AF and equalizer matrices are optimized jointly. The CFs are again those of Equations (13), (15), (16), (22), i.e the same as in Section III for various constellations. The optimization problem of the SRD link design can be stated as,

$$\mathbf{A}_S^{mber}, \mathbf{A}_F^{mber}, \mathbf{W}_d^{mber} = \underset{\mathbf{A}_S, \mathbf{A}_F, \mathbf{W}_d}{arg} \min\ P_e(\mathbf{A}_S, \mathbf{A}_F, \mathbf{W}_d)$$
$$s.t\ (1)\ Tr\left\{\mathbf{A}_F\left(\sigma_x^2 \mathbf{H}_{sr}\mathbf{H}_{sr}^H + \sigma_r^2 \mathbf{I}_{N_r}\right)\mathbf{A}_F^H\right\} \le P_r$$
$$(2)\ \sigma_x^2 Tr\left\{\mathbf{A}_S^H \mathbf{A}_S\right\} \le P_t, \quad (23)$$

where P_t is the transmit power limit. Additionally, we also consider a suboptimal structure for $\mathbf{A}_S$ for the case of reducing the number of variables during the optimization process. We consider the SVD of $\mathbf{A}_S$ with $\mathbf{A}_S = \mathbf{V}_1\mathbf{\Sigma}_S$, where $\mathbf{V}_1$ is from the SVD decomposition of $\mathbf{H}_{sr}$ and $\mathbf{\Sigma}_S$ is a diagonal matrix having the singular values. We also use the parallel optimization of $P_{e,i}$, as formulated in Section III. With these suboptimal approaches in mind, the optimization problem can be restated as,

For $\mathrm{i} = \mathrm{k}$:
$$\mathbf{\Sigma}_S^{mber}, \mathbf{\Sigma}_F^{mber}, \mathbf{w}_k^{mber} = \underset{\mathbf{\Sigma}_S, \mathbf{\Sigma}_F, \boldsymbol{w}_k}{arg} \min\ P_{e,k}(\mathbf{\Sigma}_S, \mathbf{\Sigma}_F, \mathbf{w}_k)$$
$$s.t\ (1)\ \sum_{i=1}^{N_r}\sigma_{f,i}^2\left(\sigma_x^2\sigma_{sr,i}^2 + \sigma_r^2\right) \le P_r,$$
$$(2)\ \sigma_x^2\sum_{i=1}^{N_s}\sigma_{s,i}^2 \le P_t. \quad (24)$$

For $\mathrm{i} = 1, 2, \ldots, \mathrm{k}-1, \mathrm{k}+1, \ldots, N_x$:
$$\mathbf{w}_i^{mber} = \underset{\boldsymbol{w}_i}{arg}\min\ P_{e,i}\left(\mathbf{\Sigma}_S^{mber}, \mathbf{\Sigma}_F^{mber}, \mathbf{w}_i\right), \quad (25)$$

where $\sigma_{s,i}$ represents the singular value of $\mathbf{A}_S$.

V. Solution of the MBER Optimization Problem

Remarks on CF

The MBER CF may have multiple local minima. As for example, Fig. 2. plots a CF with respect to the equalizer weights (Only the first equalizer $\mathbf{w}_1$) for $N_s = N_r = N_d = 2$ for a fixed real-valued channel and for fixed real-valued $\mathbf{A}_F$ and $\mathbf{A}_S$ matrices for the BPSK signal sets. The equalizer length is 2. For this example, the real-valued channels are assumed to be $\mathbf{H}_{sr} = \begin{bmatrix} -1.12 & 0.74 \\ 0.41 & 0.90 \end{bmatrix}$ and $\mathbf{H}_{rd} = \begin{bmatrix} -1.53 & -0.86 \\ 0.51 & -0.38 \end{bmatrix}$. Observe in Fig. 2 that the CF has several minima with respect to the equalizer weight $\mathbf{w}_1$, hence conventional gradient-based receivers might get stuck in a local optimum, depending on where the search is started on this surface. It is also noted that the solutions obtained from both the MBER and the LMMSE methods are different ((3.4, 8.2) and (5.2, 9.4) for MBER and LMMSE, respectively), while the CF values are 7.8×10^{-3} and 1.1×10^{-2} for MBER and LMMSE methods, respectively. The LMMSE solution might be a reasonable starting point [17].

Binary Genetic Algorithm: Fortunately, random guided optimization methods, like Genetic Algorithms (GA) [21], Simulated Annealing (SA) [24] etc. are capable of circumventing this problem. In this work, we used the binary GA for finding $\mathbf{W}_d$, $\mathbf{A}_F$. As this GA accepts only real-valued variables, we form a vector $\mathbf{v} \in \mathbb{R}^{(N_d N_x + N_r N_s + N_r^2)\times 1}$ by stacking all the real and imaginary components of the $\mathbf{W}_d$, $\mathbf{A}_F$, $\mathbf{A}_S$ matrices as follows

$$\mathbf{v} = [\Re\{vec(\mathbf{W}_d)\}\,\Im\{vec(\mathbf{W}_d)\}\,\Re\{vec(\mathbf{A}_S)\}$$
$$\Im\{vec(\mathbf{A}_S)\}\,\Re\{vec(\mathbf{A}_F)\}\,\Im\{vec(\mathbf{A}_F)\}]^T. \quad (26)$$

Similarly, for the case of the suboptimal scenario, we would form the vector as

$$\mathbf{v} = [\Re\{vec(\mathbf{w}_k)\}\{vec(\mathbf{\Sigma}_S)\}\{vec(\mathbf{\Sigma}_F)\}]^T. \quad (27)$$

The vector $\mathbf{v}$ is first converted to a binary string and then a series of GA operations like "Parents selection", "Crossover" and "Mutation" are invoked [21] for finding an improved

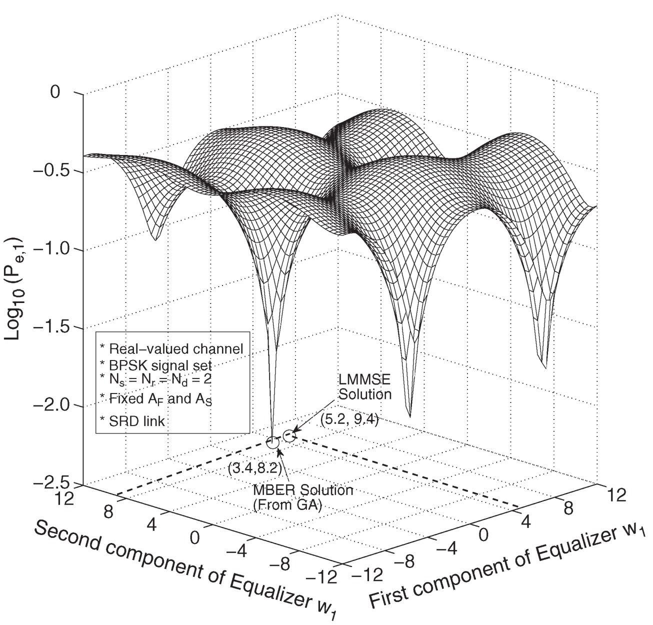

Fig. 2. Logarithm of CF from Equation (11) is plotted with respect to the first equalizer $\mathbf{w}_1$. Equalizer $\mathbf{w}_1$ is real-valued and is of the length 2. $N_s = N_r = N_d = 2$ are associated with fixed $\mathbf{A}_F$ and $\mathbf{A}_S$ matrices and fixed real-valued channel. The signal set is assumed to be BPSK. The MBER solution (obtained from GA) of $\mathbf{w}_1$ is (3.4, 8.2), while its LMMSE solution is (5.2, 9.4). The value of CF at the MBER solution is 7.8×10^{-3}, while it is 1.1×10^{-2} at the LMMSE solution.

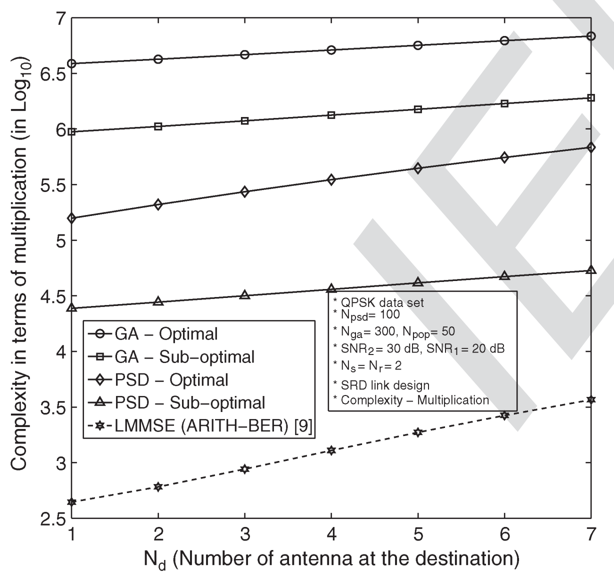

Fig. 3. Complexity (in terms of multiplication) vs. N_d comparison with various optimization options for SRD link design fixing $N_r = 2$, $N_s = 2$, $N_s = N_x$ and QPSK data set.

solution. This binary string is also known as a chromosome. We initially "seed" the GA with an initial solution constituted by the LMMSE one, so that the GA achieves a faster convergence. Unlike any steepest descent method, GA would search through various possible minima using "evolutionary" techniques. Thus, it has a reduced chance of getting into a local minimum compared to the case of completely random initialization. We provide a brief description of the GA in Appendix I. The procedure conceived for finding $\mathbf{A}_F$, $\mathbf{W}_d$ and $\mathbf{A}_S$ with the aid of our constrained binary GA is given in Algorithm. 1.

Algorithm 1: MBER based $\mathbf{A}_F$, $\mathbf{W}_d$ and $\mathbf{A}_F$ design for the relay link (Suboptimal).

1: **Given**: N_s, N_r, N_d, $\mathbf{H}_{sr}$, $\mathbf{H}_{rd}$ with SVD components σ_x^2, σ_r^2, σ_d^2 and P_r along with LMMSE solutions of $\mathbf{W}_d$, $\mathbf{A}_F$ and $\mathbf{A}_S$ as initial "seed".
2: Obtain $\mathbf{\Sigma}_F^{mber}$, $\mathbf{w}_k^{mber}$ from Equation (11) using our constrained binary GA.
3: **for** $i = 1, 2, \ldots, k-1, k+1, \ldots, N_x\}$
4: Substitute $\mathbf{\Sigma}_F^{mber}$ calculated for $i = k$ into $P_{e,i}$.
5: Find $\mathbf{w}_i^{mber}$ from Equation (12) using our binary GA.
6: **end for**
7: **return**$\mathbf{w}_i^{mber}$ for $i = 1, \ldots, N_x$ and $\mathbf{\Sigma}_F^{mber}$, $\mathbf{\Sigma}_S^{mber}$.

Projected Steepest Descent method: We have also used techniques, the low-complexity Projected Steepest Descent (PSD) [22] optimization method, which is one of the steepest descent conceived for constrained optimization [22]. We first form a vector of all the variables of interest. In the case of the optimal scenario, we stack all the complex components of the $\mathbf{W}_d$, $\mathbf{A}_F$ and $\mathbf{A}_S$ matrices to form $\mathbf{v} \in \mathbb{C}^{(N_d N_x + N_r^2 + N_s N_r) \times 1}$ (the variable of interest) as follows

$$\mathbf{v} = \left[\{vec(\mathbf{W}_d)\} \{vec(\mathbf{A}_F)\} \{vec(\mathbf{A}_S)\} \right]^T. \tag{28}$$

For the PSD method, the updated vector at the jth iteration is obtained as

$$\mathbf{v}_{j+1} = \mathbf{v}_j + \alpha \mathbf{s}_j - \mathbf{G}_j \left(\mathbf{G}_j^H \mathbf{G}_j \right)^{-1} \mathbf{g}_j \tag{29}$$

where $\mathbf{G}_j$ is the gradient of the feasible constraints, $\mathbf{g}_j$ is the stack of feasible constraints and can be defined as follows

$$\mathbf{g}_j = \begin{bmatrix} \left(Tr\left(\mathbf{A}_F \left(\sigma_x^2 \mathbf{H}_{sr} \mathbf{H}_{sr}^H + \sigma_r^2 \mathbf{I}_{N_r} \right) \mathbf{A}_F^H \right) - P_r \right) \\ \left(\sigma_x^2 \left(Tr\left(\mathbf{A}_S^H \mathbf{A}_S \right) \right) - P_t \right) \end{bmatrix} \tag{30}$$

We also define $\mathbf{s}_j$ as follows

$$\mathbf{s}_j = -\left[\mathbf{I} - \mathbf{G}_j \left(\mathbf{G}_j^H \mathbf{G}_j \right)^{-1} \mathbf{G}_j^H \right] \nabla f(\mathbf{x}_j). \tag{31}$$

along with $\alpha = -(\gamma f(\mathbf{x}_j) / \mathbf{s}_j^H \nabla f(\mathbf{x}_j))$, where γ is the desired reduction factor, usually assumed to be 0.05 (5%). For our specific problem with the optimal case, $\mathbf{G}_j$ will be obtained as follows

$$\mathbf{G}_j = \begin{bmatrix} vec\left(\mathbf{0}_{N_d \times N_x}\right) & vec\left(\mathbf{0}_{N_d \times N_x}\right) \\ vec\left(\mathbf{A}_F \mathbf{A}_1\right) & vec\left(\mathbf{0}_{N_r \times N_r}\right) \\ vec\left(\mathbf{0}_{N_s \times N_s}\right) & vec\left(\mathbf{A}_S\right) \end{bmatrix} \tag{32}$$

where $\mathbf{A}_1 \triangleq (\sigma_x^2 \mathbf{H}_{sr} \mathbf{H}_{sr}^H + \sigma_r^2 \mathbf{I}_{N_r})(\sigma_x^2 \mathbf{H}_{sr} \mathbf{H}_{sr}^H + \sigma_r^2 \mathbf{I}_{N_r})^H$. For the suboptimal case, $\mathbf{G}_j$ would be obtained as follows

$$\mathbf{G}_j^{sub} = \begin{bmatrix} vec\left(\mathbf{0}_{N_d \times 1}\right) & vec\left(\mathbf{0}_{N_d \times 1}\right) \\ \mathbf{c}_1 & vec\left(\mathbf{0}_{N_r \times 1}\right) \\ vec\left(\mathbf{0}_{N_x \times 1}\right) & \mathbf{c}_2 \end{bmatrix} \tag{33}$$

TABLE II
COMPUTATION COMPLEXITY COMPARISON BETWEEN THE PROPOSED MBER METHOD WITH LMMSE METHOD FOR SRD RELAY

Algorithm	MBER Complexity
GA (Multiplication) (Optimal)	$N_{pop}N_{ga}(4N_rN_d(N_r+N_s)$ $+4N_rN_sN_x+4N_dN_r^2+2N_d^2$ $+N_x(4N_d^2+4N_d)+4N_dN_sN_x+8N_r^3$ $+2N_xM^{N_x}(4N_x+1+N_Q)+4N_r^2N_s$ $+2N_r^2+4N_s^2N_x+1)$
GA (Total operations) (Optimal)	$N_{pop}N_{ga}(2N_d(N_r+N_s)(4N_r-1)$ $+(8N_s-2)N_rN_x+(8N_r-2)N_rN_d$ $+2N_d^2+N_d+N_x(8N_d^2+6N_d-2)$ $+4N_dN_sN_x+2N_xM^{N_x}(4N_x+1+N_Q)$ $+N_r^2(8N_s+16N_r-6)+2N_r$ $+2(N_r-1)+(8N_s-2)N_sN_x-1$
GA (Multiplication) (Sub-optimal)	$N_{pop}N_{ga}(3\min(N_d,N_r,N_s,N_x)$ $+2N_dN_x+4N_dN_r^2+2N_d^2$ $+N_x+N_x(4N_d^2+4N_d)+4N_dN_sN_x$ $+2N_xM^{N_x}N_Q+2N_r+1)$
GA (Total operations) (Sub-optimal)	$N_{pop}N_{ga}(3\min(N_d,N_r,N_s,N_x)$ $+2N_dN_x+(8N_r-2)N_rN_d+2N_d^2$ $+N_x(8N_d^2+6N_d-2)+4N_dN_sN_x$ $+2N_xM^{N_x}N_Q+3N_r+N_s+1+N_d)$

where $[\mathbf{c}_1]_i = (\sigma_x^2\sigma_{sr,i}^2 + \sigma_r^2)$ and $[\mathbf{c}_2]_i = \sigma_x^2$. For suboptimal case, $\mathbf{g}_j$ is defined as follows

$$\mathbf{g}_j^{sub} = \begin{bmatrix} \left(\sum_{i=1}^{N_r} \sigma_{f,i}^2(\sigma_x^2\sigma_{sr,i}^2+\sigma_r^2) - P_r\right) \\ \left(\sigma_x^2 \sum_{i=1}^{N_s} \sigma_{s,i}^2 - P_t\right) \end{bmatrix} \tag{34}$$

For all cases, the initial value of $\mathbf{v}$ is chosen from the LMMSE solution.

VI. COMPUTATIONAL COMPLEXITY ANALYSIS

Let us now approximate the computational complexity of the relay link designs using the MBER CF. We express it in terms of the number of operations, which can be addition, subtraction and multiplication operations. We first quantify the complexity in terms of the number of multiplications and then in terms of all the operations. We found that the complexity is dominated by the multiplications due to the associated matrix operations. We have also considered the complexity separately for both the optimal and sub-optimal approaches. Let us assume that N_{pop} and N_{ga} are the population size and the average number of GA iterations, respectively. The complexity results are presented in Table II for the SRD case. However, the details of the analysis are given in Appendix II along with the RD case as well. We have also analyzed the detailed complexity involving the PSD optimization, albeit they are not given in the table due to space limitations.

Notes:

1) An approximation for N_Q can be obtained in several ways. In practice, the $Q(\cdot)$-function is calculated using the look-up table. Ignoring the off-line calculations of its values at various data points, we need to compute the index of the discretized argument, which needs one unit of operation followed by a memory-read. The other approach is constituted by the more accurate Taylor series.

$$Q(x) = \frac{1}{2} - \frac{1}{\sqrt{2\pi}} \sum_{n=0}^{\infty} \frac{(-1)^{(n)} x^{2n+1}}{n!(2n+1)2^n}. \tag{35}$$

We note that typically $2n$ is calculated by the left-shifting of the binary string by one position and 2^n is simply a binary number of length $(n+1)$ with only a single '1' at the $(n+1)^{th}$ position. Thus, we can ignore the complexity involving these two operations. Now, we can calculate the N_Q as $N_Q \approx 4N_{lim}$ with multiplications and $N_Q \approx 5N_{lim}$ with total operations, respectively, where N_{lim} is a number for representing the limit of Taylor series sum. Simulation shows that even $N_{lim} \geq 20$ gives a good approximation with argument $x \leq 4$.

2) In the complexity analysis, another complexity component involving the SVD decomposition of a matrix has to be mentioned, which is required for both the LMMSE algorithm and for our proposed low complexity solution. For the channel matrices $\mathbf{H}_{sr}$ and $\mathbf{H}_{rd}$, the order of complexity will be $O(4N_r^2N_s+22N_s^3)+O(4N_d^2N_r+22N_r^3)$.

3) The computational complexity of the LMMSE solution relying on ARITH-BER [9] has not been analyzed in [9], hence we analyze it for comparison. The complexity in terms of the multiplications is approximately $4N_s^2N_x + 8N_s + 4 + 19N_s + 2N_r + 4N_r^3 + 4N_r\, N_s^2 + (32N_s^3 - 12N_s^2 - 2N_s)/6 + 3\min(N_d, N_s, N_r, N_x) + 2N_dN_x + (32N_d^3 - 12N_d^2 - 2N_d)/6 + 4N_dN_r^2 + 2N_d^2 + 4N_dN_sN_x + 4N_sN_d^2 + 2N_sN_d$. The total complexity is approximately $(8N_s-2)N_sN_x + 29N_s + 3 + (8N_r-2)N_r^2 + 2N_r + (8N_s-2)N_rN_s + (32N_s^3 + 60N_s^2 - 14N_s)/3 + (8N_s - 2)N_dN_x + (8N_d-2)N_sN_d + 2N_sN_d + 4N_d^2 + (32N_d^3 + 60N_d^2 - 14N_d)/3 + 3\min(N_d, N_r, N_s, N_x)2N_dN_x + (8N_r-2)N_rN_d + N_d$.

VII. NUMERICAL RESULTS

Let us now study the BER performance of the proposed method against that of the LMMSE method [7]. Our simulations are performed in two stages. During the first stage, we use a known training sequence for determining both the TPC as well as the AF and equalizer matrices of the SN, RN, DN respectively. In the second stage, the data sequence is detected. We consider a flat Rayleigh fading i.i.d channel with unit variance for each complex element of $\mathbf{H}_{sr}$ and $\mathbf{H}_{rd}$. Thus, the Channel Impulse Response (CIR) is a non-dispersive Rayleigh-faded one. Most of the simulations are preformed for $N_s = 2$, $N_r = 2$, $N_d = 2$ with channel coding, which uses Convolution Code (CC) of $(7,5)_8$. We have used the Soft-Output Viterbi decoding [23]. The RN's SNR is defined as $\mathrm{SNR}_1 = 10\log_{10}((\sigma_x^2/\sigma_1^2))$ dB, where σ_x^2 is the power of each x_i, which is set to (P_t/N_x) with $P_t = 1$ dBm. The DN's SNR is defined as $\mathrm{SNR}_2 = 10\log_{10}((P_r/N_r\sigma_2^2))$ dB, with the RN power constraint of $P_r = 5$ dBm. Finally the SN's power is constrained to $P_t = 1$ dBm unless specified otherwise. The SNR_1 is kept at 20 dB. Our simulation results are averaged

TABLE III
GA PARAMETERS

Parameters	*Values*
Population Size	50
GA maximum iteration limit	500
Mutation Type	Bit flipping
Probability of mutation	0.01
Binary string length per variable	16 bit
Initialization	LMMSE
Crossover type	Single point

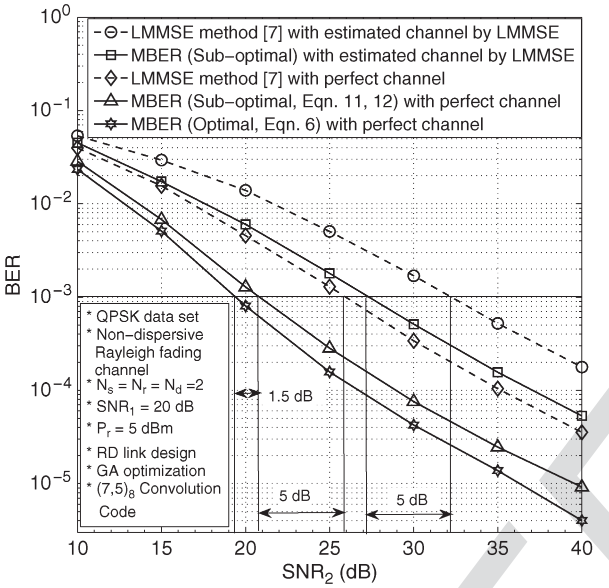

Fig. 4. BER vs. SNR_2 performance of the RN-DN link design based on the MBER method (with full $\mathbf{A}_F$, $\mathbf{W}_d$ (equation (6)) and suboptimal methods (equations (11) and (12)) along with the LMMSE method over a flat Rayleigh fading channel. Performances with and without the channel estimation are presented. $N_s, N_r, N_d = 2$, P_r is constrained to 5 dBm and SNR_1 is 20 dB. Convolution code of $(7,5)_8$ is used along with the GA optimization.

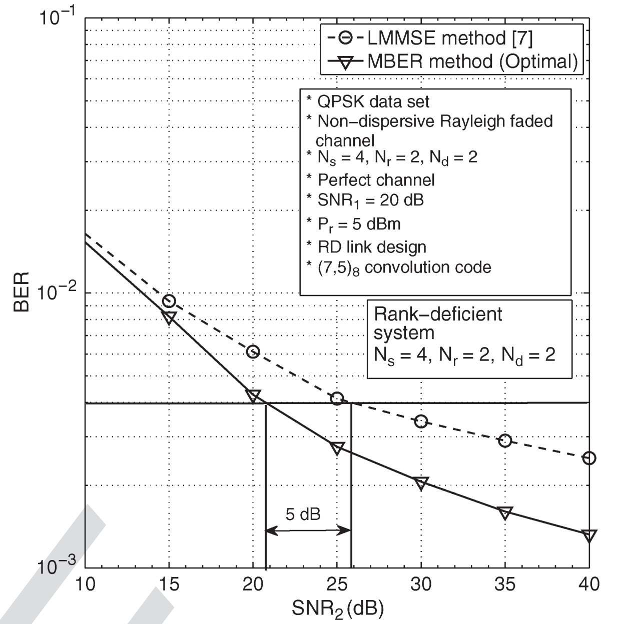

Fig. 5. BER vs. SNR_2 performance of the rank-deficient RN-DN link design based on the MBER method (optimal) along with the LMMSE method over a flat Rayleigh fading perfect channel. $N_s = 4$ and $N_r, N_d = 2$, P_r is constrained to 5 dBm and SNR_1 is 20 dB. Convolution code of $(7,5)_8$ is used along with the GA optimization.

over 1000 channel realizations per SNR value. In all our simulation setup, we have assumed $N_x = N_s$, though any value of N_x can be assumed. The GA related parameters are chosen as per Table III.

Experiment 1: This experiment is for the RD link design. The primary focus of this experiment is to characterize the BER performance of the proposed MBER method against that of the LMMSE benchmark [7]. We have also evaluated the BER performance both with perfect and with estimated channel, where the channel was also estimated using the LMMSE technique. In the second part of the experiment, we characterized the various suboptimal methods along with the original problem formulation of Equation (6) for analyzing the effects of $\mathbf{A}_F$ and $\mathbf{W}_d$. In this experiment, we have also shown the superiority of the MBER method over a rank-deficient system, where conventional LMMSE technique fails to perform adequately.

Remarks:

1) Fig. 4. plots the BER vs. SNR_2 performance of both the MBER and LMMSE based RD link design. Observe in Fig. 4 that as the SNR increases, the MBER method increasingly outperforms the LMMSE method. At $\text{BER} = 10^{-3}$ the MBER method requires an SNR of approximately 19.5 dB (suboptimal, SVD based) and 20.7 dB (optimal), respectively, while the LMMSE method needs SNR $\approx$ 26 dB for the perfectly known channel. Thus, the MBER method attains an SNR gain of approximately 5 dB (suboptimal) and 6.5 dB (optimal), respectively for the scenario of $\text{SNR}_1 = 20$ dB and $P_r = 5$ dBm. The SNR gain of the LMMSE-estimated channel remains almost ≥ 5 dB for the suboptimal MBER based RN-DN link design.
2) Fig. 5 shows the BER performance of a rank-deficient system. The $N_s = 4$ with $N_r = 2N_d = 2$. It shows that at $\text{BER} = 4 \times 10^{-3}$, the MBER method gives a BER gain of almost 5 dB, where conventional LMMSE method fails to perform adequately.
3) Let us now consider both the SVD structure of $\mathbf{A}_F$ and its original non-decomposed structure. In both the cases, we generate $\mathbf{w}_i$ in both ways, first as in Equation (6) and then as in Equations (11) and (12). Fig. 6 characterizes all these cases. Observe that at $\text{BER} = 10^{-3}$, the SVD structure based $\mathbf{A}_F$ obtains a degraded SNR performance of 1.5 dB compared to the case, where $\mathbf{A}_F$ assumes no SVD structure. It is also observed from Fig. 6 that the two choices for determining the equalizer matrix $\mathbf{W}_d$ do not have severe impact on the performance. This implies that $\mathbf{A}_F$ dominates the CF compared to the equalizer matrix $\mathbf{W}_d$ in the MBER framework. This also highlights the fact that our low-complexity solution of Equations (11) and (12) conceived for determining the DN's equalizers in parallel does not impose any substantial degradation on the BER performance in Fig. 6.

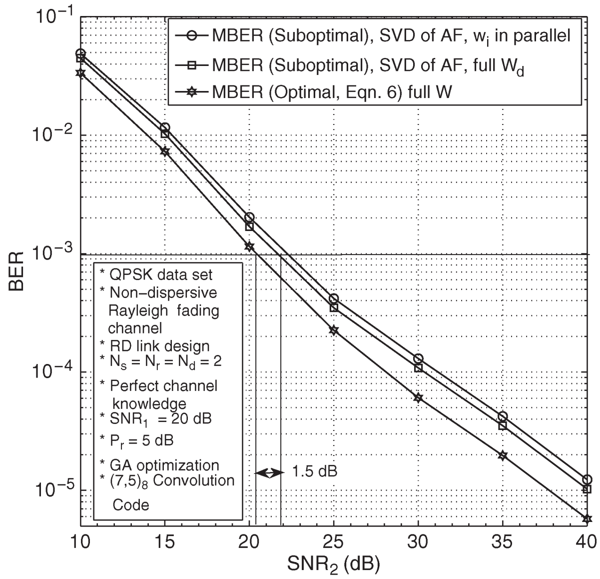

Fig. 6. BER vs. SNR_2 performance of the RD link design based on the MBER method with various options for $\mathbf{A}_F$ and $\mathbf{W}_d$ matrices (Various combinations of equations (6) and (11), (12)) with a flat Rayleigh fading channel. Channels are perfectly known. $N_s, N_r, N_d = 2$, P_r is constrained to 5 dBm and SNR_1 is 20 dB with CC code of $(7, 5)_8$.

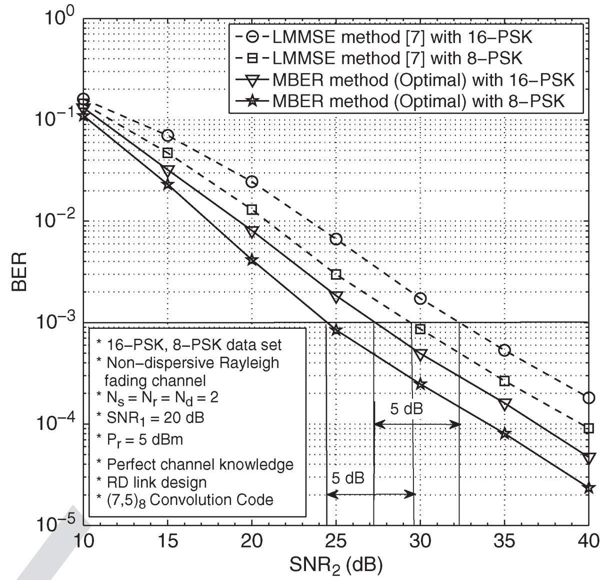

Fig. 7. BER vs. SNR_2 performance of the RD link design based on the MBER method over a flat Rayleigh fading channel with 8- and 16-PSK signal sets with CC code of $(7, 5)_8$. Channels are perfectly known. $N_s, N_r, N_d = 2$ with P_r and SNR_1 being constrained to 5 dBm and 20 dB, respectively.

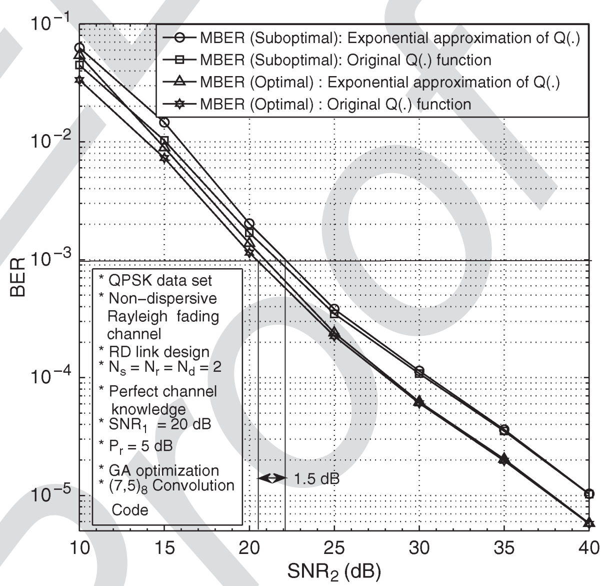

Fig. 8. BER vs. SNR_2 performance of the RD link design based on the MBER method with the Gaussian error function $Q(.)$-function approximation to an exponential one over a flat Rayleigh fading channel. Channels are perfectly known. QPSK signal set is used with CC code of $(7, 5)_8$. $N_s, N_r, N_d = 2$ with P_r being constrained to 5 dBm.

Experiment 2: Thi experiment characterizes the BER performance of both 8-PSK and 16-PSK relying on the MBER CF for transmission over a flat Rayleigh fading channel for the RD link. The channels are assumed to be perfectly known. The rest of the experimental setup is the same as in Experiment-1. *Remarks*:

1) Fig. 7 plots the BER of the MBER method for both 8-PSK and 16-PSK. Observe in Fig. 7 that at the BER $= 10^{-3}$ 8-PSK using the MBER CF requires an SNR of approximately 24.5 dB (suboptimal, SVD), while the LMMSE method needs approximately 29.5 dB. Thus, the MBER method provides an SNR gain of approximately 5 dB (suboptimal) in conjunction with $\text{SNR}_1 = 20$ dB and $P_r = 5$ dBm for 8-PSK. Similar BER improvements are attained also for 16-PSK.

Experiment 3: In this experiment, the Gaussian $Q(\cdot)$-function encapsulated in the CF is approximated by the less complex function of $Q(x) \approx (1/2)e^{-x^2/2}$[23]. In Fig. 8, we only characterize the RD link, this investigation may be readily extended to the SRD link design as well. Again, the channels are assumed to be perfectly known in this experiment. *Remarks*:

1) Fig. 8 portrays the BER performance of the MBER method using the above-mentioned $Q(x) \approx (1/2)e^{-x^2/2}$ approximation for the RD link, which reduces the complexity of the search from that of Equation (11) to Equation (12) imposed, when finding $\mathbf{A}_F$ and $\mathbf{W}_d$. Observe in Fig. 8 that the performance penalty imposed by this approximation is negligible at higher SNR values (> 25 dB), although at lower SNR values this degradation is non-negligible.

Experiment 4: In this experiment we consider the SRD link using our proposed MBER based framework. We have also considered a $4 \times 2 \times 2$ rank-deficient SRD case. We set the SN and RN power constraints to be $P_t = 5$ dBm and $P_r = 5$ dBm, respectively. We do not invoke the SVD of the $\mathbf{A}_F$ and $\mathbf{A}_S$ matrices in this experiment. The channels are assumed to be perfectly known. We have used CC code of $(7, 5)_8$. In this experiment, we have used both GA with LMMSE "seed" and PSD with LMMSE initial solution. *Remarks*:

1) Fig. 9 characterizes the BER performance of the SN-RN-DN link using our MBER framework. With GA method, at the BER $= 10^{-3}$, the MBER method requires an SNR

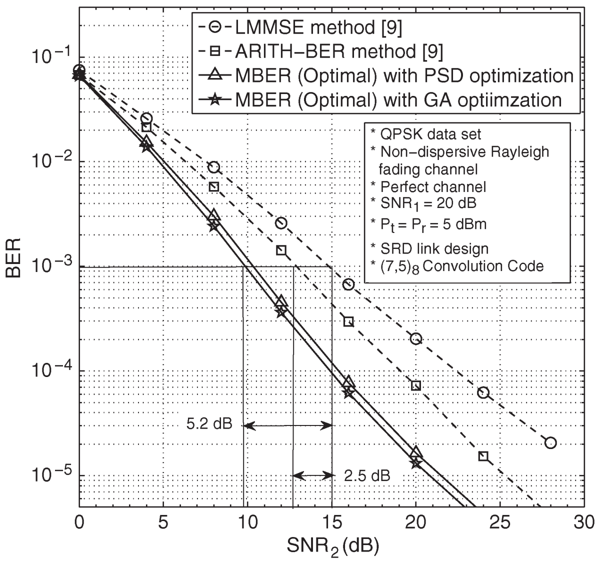

Fig. 9. BER vs. SNR_2 performance of the SRD link design based on the MBER method over a flat Rayleigh fading channel. Channels are perfectly known. $N_s, N_r, N_d = 2$, P_r and P_t are constrained to 5 dBm and SNR_1 is 20 dB. QPSK signal set is used with CC code of $(7,5)_8$. GA and PSD optimizations are used.

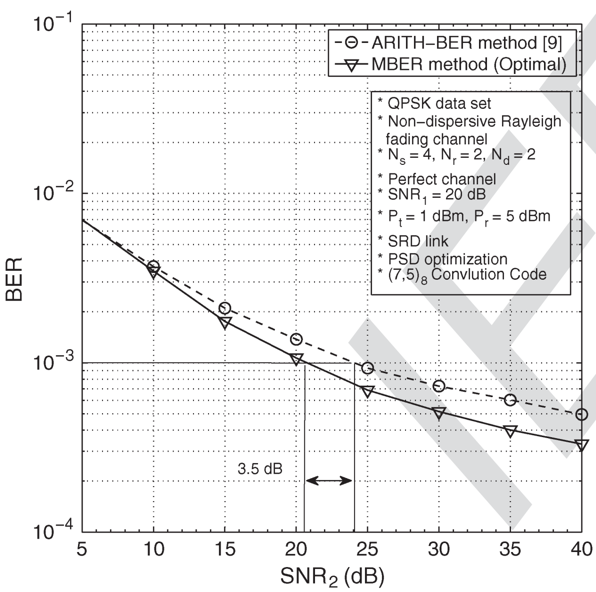

Fig. 10. BER vs. SNR_2 performance of a rank-deficient $4 \times 2 \times 2$ SRD link design based on the MBER method over a flat Rayleigh fading channel. Channels are perfectly known. $N_s = 4$, $N_r, N_d = 2$, P_r and P_t are constrained to 5 dBm and SNR_1 is 20 dB. QPSK signal set is used with CC code of $(7,5)_8$. PSD optimization is used.

of approximately 9.8 dB (optimal), while the LMMSE method needs 15 dB and ARITH-BER requires 13.5 dB, respectively. Thus, the MBER method attains an SNR gain of approximately 5.2 dB and 3.7 dB for the SRD link with respect to LMMSE and ARITH-BER, respectively. We observe that PSD gives a 0.7 dB SNR degradation.

2) Fig. 10 shows the BER performance of the rank-deficient case. It shows that we can still attain an SNR gain of almost 3.5 db at the BER $= 1 \times 10^{-3}$ with coded data along with the PSD optimization method.

VIII. Conclusions

New MBER-based TPC, AF and equalizer matrices were designed for the RN-DN link and SN-RN-DN links. The CFs of various constellations were derived and a solution was found for the design of these matrices using the MBER framework. Sub-optimal approaches have also been proposed for computational complexity reduction. It was shown that the BER performance of the proposed method is superior compared to the LMMSE method, albeit this improved performance has been achieved at an increased computational complexity.

Appendix I
Optimization Techniques

In this contribution, we have adopted two optimization methods, namely the binary GA [21] and the PSD [22]. Below we provide a brief description of the GA technique in the context of our problem.

A. Binary GA

The binary GA is a heuristic method of optimization [21]. We form a vector also referred to as a chromosome from the variables of interest by stacking all the variables' real and imaginary components as defined in Equation (26).

1) *Population selection* GA commences its operation from a set of initial chromosome values known as the initial population having a size of N_{pop}. The initial solution can be randomly generated or "seeded" with a better initial choice. The second option leads to a faster convergence. In our case, the "seed" is the "LMMSE" solution and the initial population is generated with the aid of a slight random variation around the "seed". Now, for every chromosome in the population, a "fitness" value is obtained by calculating the CF value against each of them. Then, the Roulette-Wheel algorithm of [21] is invoked for selecting the suitable parent solutions for generating child solutions for the next iteration. A pair of techniques referred to as crossover and mutation are invoked for generating children from the parents.
2) *Crossover* The crossover operation is a chromosome "reproduction" technique by which an off-spring is generated upon picking various parts of its parent chromosome. This method introduces a large amount of characteristic variation into the off-spring. Let us consider the following example. Let us assume that a random binary string, $B1$, which has the same length as chromosome is created. We also assume that two children, namely $Ch1$ and $Ch2$ have to be created from two parent chromosomes $P1$ and $P2$. Then, if the ith position of $B1$ is 0, $Ch1$ and $Ch2$ would fill up their ith position from the ith position of $P1$ and $P2$, respectively. Otherwise, the ith position of $P1$ would populate $Ch2$ and that of $P2$ would go to $Ch1$.

$$P1 = [11000110];$$
$$P2 = [10111001];$$
$$B1 = [00101011]; \tag{36}$$

Hence, the children become

$$\begin{aligned} Ch1 &= [11101101];\\ Ch2 &= [10010010]; \end{aligned} \tag{37}$$

Mutation Mutation is a relatively small-scale characteristic variational "reproduction" tool for off-spring generation. It introduces a bit flipping at a few randomly selected places of the chromosomes. For example, if a parent chromosome is $P = [11000110]$, a mutation at the 2nd Least-Significant-Bit (LSB) position generates a child $Ch = [11000100]$.

3) *Termination* Using the crossover and mutation techniques, a new set of off-spring is generated along with their fitness value. If one of them satisfies the required fitness value, the process is terminated with that chromosome being the solution. The process is also terminated, if the maximum number of iterations is exceeded. If no sufficiently good fit is found at a given iteration (provided the maximum iteration number has not been reached), the algorithm goes ahead with the selection of parents from the current set of children using the Roulette-Wheel algorithm mentioned earlier.

Appendix II
Detail Complexity Analysis

The CF of BPSK formulated in Equation (13) is considered here first for this calculation, which is readily extended to other constellations as well. However, it is noted that the overall complexity depends on the specific choice of optimization method. We first calculate the complexity of calculating the CF and constraints once, irrespective of the choice of optimization method.

RN-DN Link: Let us commence with the BPSK CF Equation (13). Let us first consider the term $(\mathbf{w}_i)^H\mathbf{H}\mathbf{x}_j x_i$. The fundamental assumption is that multiplication of two complex numbers would take 4 real data multiplication and 6 total operation (2 extra additions are required). Hence, two complex matrices of orders $\mathbb{C}^{M\times N}$ and $\mathbb{C}^{N\times K}$ would take $4MNK$ multiplications, whereas the total operation required is $(8N-2)MK$. Multiplication of a complex-valued matrix and a vector of order $\mathbb{C}^{M\times N}$ and $\mathbb{C}^{N\times 1}$ would require $4MN$ multiplications and $(8N-2)M$ total operations, respectively.

1) Thus, effective channel matrix $\mathbf{H}$ takes $N_1^m = 4N_rN_d(N_r+N_s)$ multiplications and $N_1^t = 2N_d(N_r+N_s)(4N_r-1)$ total operations respectively. Calculation of $\mathbf{H}$ is common with all the equalizers $\mathbf{w}_i$.
2) $(\mathbf{w}_i)^H\mathbf{H}\mathbf{x}_j x_i$ requires $N_2^m = 4N_dN_s + 4N_s + 1$ multiplications and $N_2^t = 8N_sN_d + 6N_d - 1$ total operations, respectively.
3) Similarly, the noise covariance matrix $\mathbf{C}_n(4)$ requires $N_3^m = 4N_dN_r^2 + 2N_d^2$ multiplications and $N_3^t = (8N_r-2)N_rN_d + 2N_d^2 + N_d$ total operations, respectively. It assumes that calculation of $\mathbf{H}_{rd}\mathbf{A}_F$ is already done with $\mathbf{H}$. Calculation of $\mathbf{C}_n$ is common with all the equalizers $\mathbf{w}_i$.
4) Thus, $\mathbf{w}_i^H\mathbf{C}_n\mathbf{w}_i$ requires $N_4^m = 4N_d^2 + 4N_d$ multiplication and $N_4^t = 8N_d^2 + 6N_d - 2$ total operations, respectively.
5) Assuming the square root and division as two unit of operations, the total complexity of calculating the CF once is $N_5^m = N_1^m + N_3^m + N_xN_4^m + 4N_dN_sN_x + N_x2^{N_x}(4N_x+1+N_Q)$ (with only multiplication) and $N_5^t = N_1^m + N_3^m + N_xN_4^t + Nx(8N_sN_d - 2Ns) + 2^{N_x}(8N_x + 1 + N_Q)$ (with total operations), respectively, where N_Q is the complexity involving the $Q(\cdot)$-function.
6) If M-QAM is chosen, the complexity will be approximately $N_5^m \approx N_1^m + N_3^m + N_xN_4^m + 4N_dN_sN_x + 2N_xM^{N_x}(4N_x + 1 + N_Q)$ with multiplication and $N_5^t \approx N_1^t + N_3^t + N_xN_4^t + 6N_s^2N_d + 2N_xM^{N_x}(2N_xN_d + 6N_d + N_Q)$ with the total complexity, respectively. For the M-PSK case with the rotated constellation concept, we need to multiply $(4N_x+1+N_Q)$ with only $2N_xM^{N_x-1}(4N_x+1+N_Q)$.
7) For the SVD-based approach, the complexity of $\mathbf{H}$ requires $N_1^m = \min(N_d,N_r) + 2N_d^2 + 4N_dN_s^2$ multiplications and $N_1^t = \min(N_d,N_r) + 2N_d^2 + (8N_s - 2)N_dN_s$ total operations.
8) Let us calculate the complexity involving the constraints. From equation (6), we obtain the complexity for constraints as $N_1^{m,c} = 8N_r^3 + 4N_r^2N_s + 2N_r^2$ with multiplication only and $N_1^{t,c} = N_r^2(8N_s + 16N_r - 6) + 2N_r + 2(N_r - 1)$ with total operations, respectively. For the SVD approach, it would be $N_1^{m,c} = 2N_r$ with multiplications and $N_1^{t,c} = 3N_r$ total operations, respectively.

SN-RN-DN Link: For the case of the SN-RN-DN link, we have to additionally incorporate the calculation of the TPC matrix $\mathbf{A}_S$.

1) We obtain the complexity for $\mathbf{H}$ as $N_1^m = 4N_rN_d(N_r + N_s) + 4N_rN_sN_x$ with multiplication and $N_1^t = 2N_d(N_r+N_s)(4N_r-1) + (8N_s-2)N_rN_x$ with total operations, respectively. For the SVD-based approach, we obtain $N_1^m = 3\min(N_d,N_r,N_s,N_x) + 2N_dN_x$ for multiplications and $N_1^t = N_1^m$ as well for the total operations.
2) An additional complexity for the source power constraint may be calculated as $N_2^{m,c} = 4N_s^2N_x + 1$ with multiplication and $N_2^{t,c} = (8N_s-2)N_sN_x + 2N_s - 1$ with total computations, respectively. For the SVD-based approach, they become $N_2^{m,c} = 1$ for multiplication and $N_2^{t,c} = N_s + 1$ for total operations, respectively.

Computational-Complexity, Specific to Optimization Method: Computational complexity is also dependent on the specific choice of optimization algorithm to determine the parameters. For binary GA, time-complexity is more appropriate. However, we try to give an approximate computational-complexity for GA. The computational-complexity for GA is dominated by the function and constraint evaluations to determine the eligible population at each iterations. Let us assume that total size of population is N_{pop} and GA requires N_{ga} iterations to converge. Then, total complexity will be approximately $N_{pop}N_{ga}(N_5^m + N_1^{m,c} + N_2^{m,c})$ with multiplication and $N_{pop}N_{ga}(N_5^t + N_1^{t,c} + N_2^{t,c})$ with total operations, respectively.

For the PSD algorithm, we need to calculate the gradient for both function and constraint. Gradient of CF is calculated numerically.

1) Gradient of CF takes $N_1^{m,psd}=2(N_dN_x+N_r^2+N_sN_r)N_5^m$ multiplication and $N_1^{t,psd}=2(N_dN_x+N_r^2+N_sN_r)N_5^t$ total operations, if we use numerical method. For the SVD-based approach, it would be $N_1^{m,psd}=2(N_d+N_x+N_r)N_5^m$ with multiplication and $N_1^{t,psd}=2(N_d+N_x+N_r)N_5^t$ with total operations.
2) Per iteration, other steps require $N_2^{m,psd}=18(N_r^2+N_sN_r)+6(N_dN_x+N_r^2+N_sN_r)+4(N_r^2+N_s^2)^2+9$ multiplications and $N_2^{t,psd}=25(N_r^2+N_sN_r)+22+10(N_dN_x+N_r^2+N_sN_r)+8(N_r^2+N_sN_r)^2$ total operations. For sub-optimal case, it would be $N_2^{m,psd}=2(N_r^2+N_s^2)+3(N_d+N_r+N_s)+1+2(N_d+N_s)$ for multiplication and $N_2^{t,psd}=6(N_r+N_s)-6+7(N_d+N_r+N_s)$ for total operations.
3) If PSD takes an average iteration of N_{psd}, the computational complexity may be approximated as $N_{psd}(N_1^{m,psd}+N_2^{m,psd})$ with multiplication and $N_{psd}(N_1^{t,psd}+N_2^{t,psd})$ with total operations.

Computational Complexity for LMMSE [9]-ARITH BER Case: We give an approximate computational complexity for the LMMSE case for comparison purpose.

1) The computation of precoder matrix $\mathbf{A}_S$ requires $4N_s^2N_x+8N_s+3$ multiplication and $(8N_s-2)N_sN_x+5N_s+1$ total operations.
2) The computation of AF matrix requires $19N_s+1+2N_r+4N_r^3+4N_rN_s^2+(32N_s^3-12N_s^2-2N_s)/6$ multiplications and $24N_s+2+(8N_r-2)N_r^2+2N_r+(8N_s-2)N_rN_s+(32N_s^3+60N_s^2-14N_s)/3$ total operations.
3) Computation of effective channel matrix and noise covariance matrix are already given.
4) Computation of equalizer matrix requires $4N_dN_sN_x+4N_sN_d^2+2N_sN_d+(32N_d^3-12N_d^2-2N_d)/6$ multiplications and $(8N_s-2)N_dN_x+(8N_d-2)N_sN_d+2N_sN_d+2N_d^2+(32N_d^3+60N_d^2-14N_d)/3$ total operations.

Acknowledgment

The financial support of the DST, India and of the EPSRC, UK under the auspices of the India-UK Advanced Technology Centre (IUATC) is gratefully acknowledged.

References

[1] Y. Rong, X. Tang, and Y. Hua, "A unified framework for optimizing linear nonregenerative multicarrier MIMO relay communication systems," *IEEE Trans. Signal Process.*, vol. 57, no. 12, pp. 4837–4851, Dec. 2009.
[2] Y. Rong, "Optimal linear non-regenerative multi-hop MIMO relays with MMSE-DFE receiver at the destination," *IEEE Trans. Wireless Commun.*, vol. 9, no. 7, pp. 2268–2279, Jul. 2010.
[3] X. J. Zhang and Y. Gong, "Adaptive power allocation for multihop regenerative relaying with limited feedback," *IEEE Trans. Veh. Technol.*, vol. 58, no. 7, pp. 3862–3867, Sep. 2009.
[4] X. J. Zhang and Y. Gong, "Jointly optimizing power allocation and relay positions for multi-relay regenerative relaying with relay selection," in *Proc. 4th ICSPCS*, 2010, pp. 1–9.
[5] J. Zou, H. Luo, M. Tao, and R. Wang, "Joint source and relay optimization for non-regenerative MIMO two-way relay systems with imperfect CSI," *IEEE Trans. Wireless Commun.*, vol. 11, no. 9, pp. 3305–3315, Sep. 2012.
[6] W. Zhang, U. Mitra, and M. Chiang, "Optimization of amplify-and- forward multicarrier two-hop transmission," *IEEE Trans. Commun.*, vol. 59, no. 5, pp. 1434–1445, May 2011.
[7] W. Guan and H. Luo, "Joint MMSE transceiver design in non- regenerative MIMO relay systems," *IEEE Commun. Lett.*, vol. 12, no. 7, pp. 517–519, Jul. 2008.
[8] C. Jeong and H.-M. Kim, "Precoder design of non-regenerative relays with covariance feedback," *IEEE Commun. Lett.*, vol. 13, no. 12, pp. 920–922, Dec. 2009.
[9] C. Song, K.-J. Lee, and I. Lee, "MMSE based transceiver designs in closed-loop non-regenerative MIMO relaying systems," *IEEE Trans. Wireless Commun.*, vol. 9, no. 7, pp. 2310–2319, Jul. 2010.
[10] C. Xing, S. Ma, and Y.-C. Wu, "Robust joint design of linear relay precoder and destination equalizer for dual-hop amplifyand- forward MIMO relay systems," *IEEE Trans. Signal Process.*, vol. 58, no. 4, pp. 2273–2283, Apr. 2010.
[11] X. Tang and Y. Hua, "Optimal design of non-regenerative MIMO wireless relays," *IEEE Trans. Wireless Commun.*, vol. 6, no. 4, pp. 1398–1407, Apr. 2007.
[12] O. Munoz-Medina, J. Vidal, and A. Agustin, "Linear transceiver design in nonregenerative relays with channel state information," *IEEE Trans. Signal Process.*, vol. 55, no. 6, pp. 2593–2604, Jun. 2007.
[13] B. Sainath and N. Mehta, "Generalizing the amplify-and-forward relay gain model: An optimal SEP perspective," *IEEE Trans. Wireless Commun.*, vol. 11, no. 11, pp. 4118–4127, Nov. 2012.
[14] T. Peng, R. de Lamare, and A. Schmeink, "Joint minimum BER power allocation and receiver design for distributed space-time coded cooperative MIMO relaying systems," in *Proc. Int. ITG WSA*, 2012, pp. 225–229.
[15] C.-C. Yeh and J. Barry, "Adaptive minimum bit-error rate equalization for binary signaling," *IEEE Trans. Commun.*, vol. 48, no. 7, pp. 1226–1235, Jul. 2000.
[16] W. Yao, S. Chen, and L. Hanzo, "Generalised vector precoding design based on the MBER criterion for multiuser transmission," in *Proc. IEEE VTC-Fall*, 2010, pp. 1–5.
[17] S. Chen, A. Livingstone, and L. Hanzo, "Minimum bit-error rate design for space-time equalization-based multiuser detection," *IEEE Trans. Commun*, vol. 54, no. 5, pp. 824–832, May 2006.
[18] W. Yao, S. Chen, and L. Hanzo, "Generalized MBER-based vector precoding design for multiuser transmission," *IEEE Trans. Veh. Technol.*, vol. 60, no. 2, pp. 739–745, Feb. 2011.
[19] W. Yao, S. Chen, and L. Hanzo, "A transceiver design based on uniform channel decomposition and MBER vector perturbation," *IEEE Trans. Veh. Technol.*, vol. 59, no. 6, pp. 3153–3159, Jul. 2010.
[20] M. Alias, S. Chen, and L. Hanzo, "Multiple-antenna-aided OFDM employing genetic-algorithm-assisted minimum bit error rate multiuser detection," *IEEE Trans. Veh. Technol.*, vol. 54, no. 5, pp. 1713–1721, Sep. 2005.
[21] D. E. Goldberg., *Genetic Algorithms in Search, Optimization, Machine Learning*. Boston, MA, USA: Addison-Wesley Longman Publishing Co., Inc, 2009.
[22] D. H. Luenberger, *Linear and Nonlinear Programming*. Englewood Cliffs, NJ, USA: Prentice-Hall, 1984.
[23] J. Proakis, *Digital Communications*., 4th ed. New York, NY, USA: McGraw-Hill, 2000.
[24] P. van Laarhoven and E. Aarts, *Simulated Annealing: Theory and Applications*. Norwell, MA, USA: Kluwer, 1987.

Amit Kumar Dutta (SM'XX) received the B.E. degree in electronics and tele-communication engineering from Bengal Engineering and Science University, India, in 2000. He is currently pursuing the Ph.D degree at the Department of ECE, Indian Institute of Science, India. AQ1

He worked in Texas Instrument (TI) Pvt. Ltd., India, from 2000 to 2009. During his career at TI, he worked on various design and test aspects of communication and entertainment related System-on-Chip. The works included digital VLSI design and its test, validation and characterization.

He is interested in the applications of statistical signal processing algorithms to wireless communication systems. His current research interests are on the various parameter estimation and signal detection for MIMO wireless receiver based on the Minimum Bit-Error-Ratio criterion.

K. V. S. Hari (M'92–SM'97) received the B.E. degree from Osmania University in 1983, M.Tech. degree from IIT Delhi in 1985, and the Ph.D. degree University of California at San Diego in 1990. Since 1992, he has been a Faculty Member at the Department of ECE, Indian Institute of Science (IISc), Bangalore, where he is currently a Professor and coordinates the activities of the Statistical Signal Processing Lab in the department. Currently, he is also an Affiliated Professor in the School of Electrical Engineering, KTH-Royal Institute of Technology, Stockholm, Sweden.

He has been a visiting faculty member at Stanford University, KTH-Royal Institute of Technology and Helsinki University of Technology (now Aalto Univ). He also worked at DLRL, Hyderabad, and at the R&D unit for Navigational Electronics, Osmania University.

His research interests are in developing signal processing algorithms for MIMO wireless communication systems, sparse signal recovery problems, indoor positioning and DOA estimation.

During his work at Stanford University, he worked on MIMO wireless channel modeling and is the coauthor of the WiMAX standard on wireless channel models for fixed-broadband wireless communication systems which proposed the Stanford University Interim (SUI) channel models. He is currently an Editor of the EURASIP's Journal on Signal Processing published by Elsevier and the Senior Associate Editor, Editorial Board of Sadhana (Indian Academy of Science Proceedings in Engineering Sciences). He is also an academic entrepreneur and is a cofounder of the company ESQUBE Communication Solutions, Bangalore.

Lajos Hanzo (F'08) received the bachelor's degree in electronics in 1976 and the doctoral degree in 1983. In 2009 he was awarded the honorary doctorate "Doctor Honoris Causa" by the Technical University of Budapest. During his 37-year career in telecommunications he has held various research and academic posts in Hungary, Germany and the UK. Since 1986 he has been with the School of Electronics and Computer Science, University of Southampton, U.K., where he holds the chair in telecommunications. He has successfully supervised more than 80 Ph.D. students, co-authored 20 John Wiley/IEEE Press books on mobile radio communications totalling in excess of 10 000 pages, published 1400+ research entries at IEEE Xplore, acted both as TPC and General Chair of IEEE conferences, presented keynote lectures and has been awarded a number of distinctions. Currently he is directing a 100-strong academic research team, working on a range of research projects in the field of wireless multimedia communications sponsored by industry, the Engineering and Physical Sciences Research Council (EPSRC) UK, the European Research Council's Advanced Fellow Grant and the Royal Society's Wolfson Research Merit Award. He is an enthusiastic supporter of industrial and academic liaison and he offers a range of industrial courses. He is also a Governor of the IEEE VTS. During 2008–2012 he was the Editor-in-Chief of the IEEE Press and a Chaired Professor also at Tsinghua University, Beijing. His research is funded by the European Research Council's Senior Research Fellow Grant. For further information on research in progress and associated publications please refer to http://www-mobile.ecs.soton.ac.uk.Dr.Hanzohasmorethan20 000+citations.

AUTHOR QUERIES

AUTHOR PLEASE ANSWER ALL QUERIES

AQ1 = Please provide membership history of author Amit Kumar Dutta.

END OF ALL QUERIES